




Article

A Long-Term Analysis of the Architecture and Operation of Water Film Cooling System for Commercial PV Modules

Vinícius Silva ^{*}, Julio Martinez, Raphael Heideier, Jonathas Bernal, André Gimenes , Miguel Udaeta 
and Marco Saidel

Energy Group of the Department of Energy and Electrical Automation Engineering of the Polytechnic School, University of São Paulo, São Paulo 05580-900, Brazil; julioromel@yahoo.com.br (J.M.); rbheideier@gmail.com (R.H.); totabernal@yahoo.com.br (J.B.); gimenes@pea.usp.br (A.G.); udaeta@pea.usp.br (M.U.); saidel@pea.usp.br (M.S.)

* Correspondence: vinicius.oliveira.silva@outlook.com.br

Abstract: This work aims at analyzing and architecting natural and artificial parameters to model a water-film cooling system for photovoltaic modules for some months under warm conditions. Methodologically, the theoretical and technical aspects were structured to develop, implement, monitor, and assess the cooling system at an on-grid, outdoor testing unit, considering the following: (i) the criteria to select and to approve the implementation site (infrastructure and climatologic and solarimetric conditions); (ii) the types, frequency and qualities of the monitored data; (iii) the system measurement, monitoring and control equipment; (iv) the commissioning of the system as a whole; and (v) the tests and results empirically obtained. The water-film cooling system reduces the temperature by 15–19%, on average, and up to a maximum of 24–35%. In terms of electric power, there was an average gain of 5–9% at the time of day with the highest solar radiation, and maximum gains of 12% on days with solar radiation above average. Regarding gross energy, average gains of 2.3–6%, and maximum gains of 6.3–12%, were obtained. It was concluded that the test unit helps understand the natural phenomena and the development, operation, and maintenance of performance gain systems of on-grid PV modules for construction on a commercial scale.

Keywords: solar energy; photovoltaic; photovoltaic cooling system; performance analysis



Citation: Silva, V.; Martinez, J.; Heideier, R.; Bernal, J.; Gimenes, A.; Udaeta, M.; Saidel, M. A Long-Term Analysis of the Architecture and Operation of Water Film Cooling System for Commercial PV Modules. *Energies* **2021**, *14*, 1515. <https://doi.org/10.3390/en14061515>

Academic Editor: Mauro Pravettoni

Received: 14 January 2021
Accepted: 19 February 2021
Published: 10 March 2021

Publisher's Note: MDPI stays neutral with regard to jurisdictional claims in published maps and institutional affiliations.



Copyright: © 2021 by the authors. Licensee MDPI, Basel, Switzerland. This article is an open access article distributed under the terms and conditions of the Creative Commons Attribution (CC BY) license (<https://creativecommons.org/licenses/by/4.0/>).

1. Introduction

The availability and use of energy are fundamental requirements for the social and economic development of any region or country [1], so much so that for a country, energy planning has as priorities the increase in energy supply in the short term and possibly in the medium term to provide these fundamental needs [2]. Solar energy is one of the renewable energy sources that has potential for applications to replace non-renewable sources of a power system [3]. Current technologies convert solar energy into electricity and heat, respectively [4]. One of the types of solar conversion technologies are photovoltaic (PV) modules. PV module heating is mainly caused by solar irradiance and ambient temperature, i.e. the periods when they are generating, reaching temperatures above 90 °C [5]. The difference in temperature between the top and bottom surface of the module can reach levels above 8.0 °C. Moreover, the junction box region concentrates the highest temperature, 37 °C, while the other areas are about 24–28 °C [6]. As for the PV cell temperature, it mainly heats on the main bus region. Therefore, the cooling system must be tilted to these regions.

Conventional PV modules [6] only produce low electricity efficiency in solar-to-electric conversion (5–22%) [7]. There are natural exogenous climatic conditions that also influence the temperature of the photovoltaic module, such as wind speed, relative humidity, solar radiation, ambient temperature and accumulated dust [8]. The increase in temperature decreases the electric efficiency of the PV module, ~0.1%/°C, with losses both by temperature (~11%) and by dirt on the surface (~7%), [9–11]. Power loss caused by temperature

increase varies in intensity, depending on the type of technology [12]. The crystalline cells suffer the highest reductions in electric power, 0.4–0.5%, [13,14]. Hence, due to the increase in temperature, not all the solar energy absorbed by the PV cells is converted into electrical energy [15].

To improve the performance of PV technologies, a wide range of technical solutions are proposed and developed in the international literature that are systematically organized and classified [15–19]. Some cooling and PV/T systems produce electricity while capturing heat [6,20]; they consist of a fluid that permeates the heat exchanger connected to the PV module, cooling the PV module and increasing its performance by 4–18% [20–22]. Depending on the type of technology, it is possible to simultaneously cool and clean the PV module [23]; this result can be obtained by open-circuit cooling systems [23–25].

There are several systems that increase the performance of electric energy generation in PV modules; the simplest one consists in directing the air stream to the bottom surface of the PV module to cool it [26–29], and the heated air can be recovered and used for internal heating [30]. Another system consists in using a heat absorber attached to the bottom surface of the PV module: through a circulating fluid, usually water, the heat is transferred from the PV module to the fluid, and can be later used—in a domestic environment—in baths and faucets [31–33]. Water is the most commonly used fluid, although other types of cooling fluid have also been used [34], such as nanofluid cooled [35–38] used in two ways (i) coolant and (ii) spectral filter [39]. However, it requires the use of specific equipment to guarantee a thermal cooling cycle, such as the Rankine cycle, which compromises electricity production gains with the reduction of the PV module temperature caused by the operation of the equipment attached to the thermodynamic cycle [40].

There are currently several types of cooling systems for PV modules, classified according to the author and level of development of the technologies [41–43], but they are mainly distributed into two major groups: (i) closed-circuit cooling system, in which the fluid circulates in a thermal collector, exchanging heat with the PV module, that is, in a confined environment [44–46]; and (ii) open-circuit cooling system, in which the fluid is directed at the PV module, running through its area in an unconfined manner, without the aid of pipes, ducts, chambers, etc., that is, in direct contact with the environment [47–53].

In this regard, it is important that mechanisms that decrease the operating temperature of the PV modules are used to increase their electric power generation performance. To that end, there must be instruments and mechanisms that allow studying and developing these technologies on a small scale for further empiric tests on scale, to reduce the development costs throughout the production and destination process of these technologies in the market. In addition, it is important to develop and to evaluate a real test unit and its empirical experiments, because although there are many works on the cooling system of PV modules, there are relatively few studies based on experimental research [54]. The literature survey revealed that, although many studies have investigated the PV/T system, there are relatively few works based on experimental research, and which demonstrate the effects and the impact of the control of its thermal and electrical parameters [26]. In addition, these experimental surveys yield results based on a few hours of measurements on a single day, and there is virtually no work showing these systems operating for weeks or months [55,56], as seen in Table A1, Appendix A.

Therefore, this work aims at systemizing and analyzing the theoretical and technical aspects for developing, implementing, monitoring, and assessing on-grid water-film cooling systems for commercial PV modules for a long period in warm conditions.

This work primarily contributes by providing a detailed empirical analysis, based on data collected in an outdoor test unit (ODTU), of the performance of cooled photovoltaic systems for a long period, using the equipment, methods and data acquisition of parameters recommended by IEC 61724. Second, it consolidates results and data, both quantitatively and qualitatively, from several works that evaluate different types of cooling systems for PV modules, demonstrating that the analysis periods are based mainly on a single day and there are practically no tests in different seasons.

The work is organized into five sections: Section 2 presents the premises for choosing the implementation site, the schematic arrangement, equipment, and components of ODTU, as well as its commissioning. Section 3 provides the results and discussions of the pre-operation and operation of the water-film, its operational characteristics, and its impact on decreasing the temperature and increasing the power generation of the PV modules over the hours, days, and months. Section 4 compares the results of the work with the results consolidated in the bibliographic review. The discussions and comparisons are presented in Tables A1 and A2. Finally, Section 5 gives the conclusions of this work.

2. Development of the ODTU

2.1. Basic Premises for the Implementation of the ODTU

The site use policies should be evaluated by the institution that will receive the ODTU, to make it easier for researchers to access the location, to go on guided tours and for the safety of the equipment and installations. In addition, it is essential to assess the existing infrastructure and the surrounding area. Thus, the following criteria were considered.

2.1.1. Accessibility

Researchers must have full access to the site, regardless of hour, day of the week or time of the year, for preventive maintenance, adjustments, and data collection and recovery. The need for urgent corrective maintenance because of occasional accidents caused by weather conditions, or any other miscellaneous accidents, must also be considered. It is recommended to determine a qualitative scale for each site, varying from difficult access to easy access, for this aspect.

2.1.2. Safety

Safety in the installations and equipment, assessing the possibility of vandalism, theft or even vulnerability to unintentional curiosity.

2.1.3. Minimum Area for Physical Installation

The outdoor test unit (ODTU) is built with structural elements that protect and support its components, such as fences, base structure and, alternatively, stays. The worst-case scenario must be considered, such as the security factor of the site that will be used, considering the hydraulic pipeline installation, electric wiring and the infrastructure of the panels and supports, besides the area for the technicians, researchers and accompanied academic visitors to move around.

2.1.4. Access to Water

The availability of a water intake channel to supply the cooling systems must be checked. A qualitative scale between easy, moderate, and hard access, was adopted.

2.1.5. Shading

The presence of buildings, walls, trees, towers, etc. that can cause shading at some hours of the day—especially to the east and west of the analyzed spot—must be checked. Barriers must be avoided; however, in case any of them are close, their position must be observed. Due to the Sun path, barriers to the south and north of the analyzed spot cause less shades than to the east and the west.

2.1.6. Grounding

The ODTU must have a lightning rod and grounding system, making it mandatory to check whether the location allows grounding of copper rods and interlinking with the lightning protection system (LPS) of the chosen site.

It is recommended to designate a qualitative scale for each location, listing whether it has LPS and grounding installations; in case it does not have them if they can be easily installed; and if it does not have them and there are technical difficulties to install them.

2.1.7. Access to the Power Grid

The main purpose of the ODTU is to test the concept of the components to increase electric power yield in PV modules. For this, the ODTU must be connected to the internal distribution grid through solar microinverters.

Therefore, it must be observed if the implementation site has access to the power grid. For each location visited, the following items are checked: (i) are there sockets? (ii) how close are the switchboards? (iii) in case there are no sockets, can they easily be installed? (iv) in case there are no switchboards, can they easily be installed? and (v) are there no sockets, making it necessary to install conduits, wires, etc.?

2.2. Shading Analysis of the Chosen Site

Figure 1 shows the disposition of the PV modules on the roof of the building, a place that minimizes the effects of shading. It also presents the location and height of 12 trees that were considered relevant for shading analysis purposes. Since the 3D modelling of the trees are uncertain, that is, they cannot be estimated with precision due to the height and excessive amount of leaves, the shading analysis was carried out in two stages: (i) considering just the buildings (where it is less uncertain); and (ii) considering every obstacle (buildings and trees). It was thus possible to assess the influence of the tree on PV modules shading, which, in a one-year period, are shaded at the beginning and end of the day (between 6:00–9:00 a.m. and 4:30–6:30 p.m.).

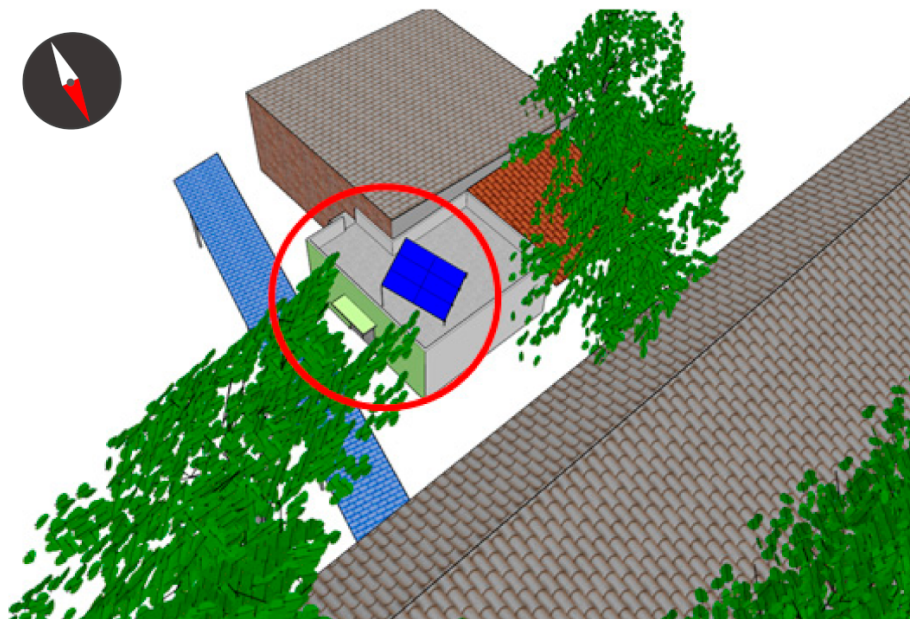


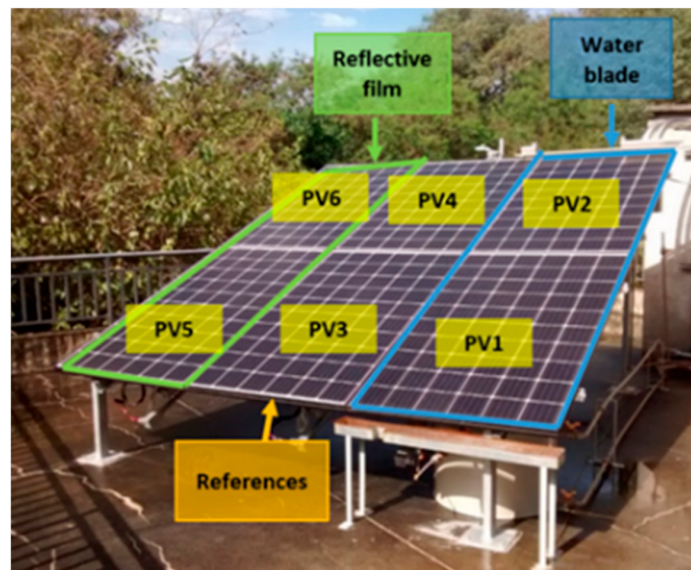
Figure 1. Representation of the ODTU implementation site—on the roof of the building and its surroundings.

2.3. ODTU Implementation

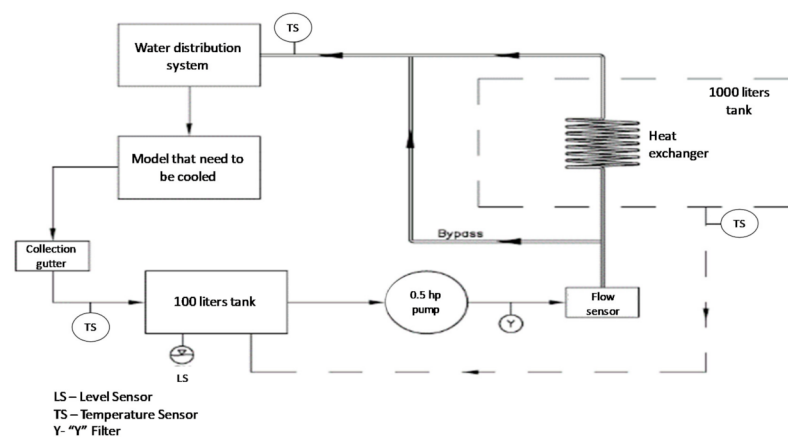
The specific-purpose ODTU is placed in the coordinates: $23^{\circ}33'24.53''$ S; $46^{\circ}43'45.47''$ W; Datum WGS84. It has an area of 45 m^2 , installed electric power of 1.65 kWp; it is composed of six (06) 275 Wp mi-Si PV modules, and it is connected to the grid in 220V/127 VAC (three-phase system). Each PV module is independently connected to a solar microinverter equipped with a Maximum Power Point Tracking (MPPT) algorithm. Two are equipped with water-film cooling system, identified as cooled PV module one (PV1) and two (PV2), two with reflective film (PV5 and PV6) [57]—not used in this work—, and two uncooled PV modules (PV3 and PV4) are used as reference PV modules, see Figure 2a.

The ODTU has: (i) one peripheric 0.5 hp pump with speed control by frequency variation [58]; (ii) one “Y” filter to remove fragments and avoid clogging the distributor;

(iii) two water tanks: one 0.1 m³ to feed the pump and to store the water after the PV modules cooling; and one 1.0 m³ tank to store a water volume that allows the operation of the system for long periods of time without having to replace the grid; (iv) two fluid supply lines: one main line with heat exchanger; and one secondary or by-pass; (v) one heat exchanger (coil) in the main line and immerse in the 1.0 m³ tank; (vi) one flushing/collection line that returns the water to the 0.1 m³ tank; (vii) one distributor to inject water on the top surface of the PV modules (water-film cooling system); (viii) one gutter for water collection, after it runs on the top surface of the PV; (ix) one panel to hold the generation and monitoring system; and (x) one panel to hold the control system of the PV modules water-film cooling system.



(a)



(b)

Figure 2. ODTU system (a) Disposition of the six PV modules; (b) Schematic arrangement of the cooling system [59].

These operating units are described in the following subitems. The schematic arrangement of the ODTU cooling system can be observed in Figure 2b.

2.4. Supervision and Monitoring System

Reliable supervision and monitoring systems are essential to guarantee the maximum performance of commercial PV plants. The detailed monitoring system is one of the

differentials between a commercial PV installation and an ODTU. The system implemented makes it possible to monitor and to store (in a local and/or remote manner) the main electric measures of the system, with a one-second sampling period, and the main thermal measures and solar radiation on a tilted surface, with a one-minute sampling period, by using individual monitoring for each of the six PV modules. It is worth highlighting that these sampling and storage rates are in accordance with the IEC Standard [60] and they also ensure a commitment between precision and cost, considering the transference and interconnection speeds of the different components of the monitoring system. Table 1 presents the parameters monitored by the monitoring system.

Table 1. Parameters monitored by the monitoring system.

Parameter	Sampling Rate	Integration Period	No. of Sensors
Solar irradiance on the inclination of the PV modules	≤1.0 min	1.0 min	01
Direct current voltage	≤1.0 s	1.0 min	06
Direct current (DC)	≤1.0 s	1.0 min	06
Active/reactive electric power in alternating current (AC) in the exit of each inverter	≤1.0 s	1.0 min	06
Neutral-phase voltage of the AC phases in the coupling point	≤1.0 s	1.0 min	03
Temperature of the PV modules	≤1.0 min	1.0 min	18
Temperature of the water in the tanks	≤1.0 min	1.0 min	02
Temperature of the water at the entrance of the flushing line	≤1.0 min	1.0 min	01
Water flow	≤1.0 min	1.0 min	01
Active electric power consumed by the water pump	≤1.0 min	1.0 min	01

2.4.1. Thermal and Electric Sensing and Monitoring

- (1) Three PT100 resistance thermometer sensors (TS) with screwable head [61]: one connected to the 1.0 m³ tank; one connected to the beginning of the flushing line (right after the gutter); and one connected to the distributor line.
- (2) 18 TS with exposed bulb type A [61], fixated on the bottom surface of the PV module. Three TS are fixed in each module, one for each arrangement of cells in series of the PV module.
- (3) Three dataloggers to obtain and to register the measured temperatures [62].
- (4) 06 DC voltage transducers [63] and 06 DC current transducers [64] to measure each PV module individually;
- (5) Two active/reactive electric power transducers (three-phase) [65] to measure the power in unbalanced charges;
- (6) One flow sensor [66] installed on the supply line to measure the instant flow of water used in the system.

2.4.2. Meteorological Sensing and Monitoring

- (1) One pyrometer [67] installed on the same tilted surface of the PV modules, in order to measure the real global solar irradiance received by the PV modules. It is a part of the ODTU, and it is connected to one of the dataloggers.
- (2) One anemometer to measure the wind speed on the location [68];
- (3) One ambient temperature sensor [69];
- (4) One barometer used to measure the local atmospheric pressure [70];
- (5) One humidity sensor installed at the ESPEL, 200 m away from the ODTU [71,72].

2.5. ODTU Commissioning

2.5.1. Visual Inspection

Before the beginning of the tests and/or assays in the specific-purpose ODTU, a visual inspection was carried out to check the implementation of the precautions and safety measures [6]. The presence of breakers, surge protection devices (SPD), residual current devices (RCD), ground conductor, etc., were confirmed. The physical integrity of the

installation components was also checked by visual inspection. None of the equipment had missing parts, signs of overheating, or any other sign that would make the integrity of each component questionable. The integrity of the connections on the electric panel, as well as the presence of durable tags to identify the circuits, was also checked. The accessibility of the ODTU facilities was also part of the visual inspection, especially regarding the generation and monitoring panel. No accessibility issues were found.

2.5.2. Operation Tests

After the previous tests and confirmations, the ODTU generation system was operated. Measurements of voltage, current and electric power were carried out on the exits of the PV modules and solar microinverters using voltmeters, ammeters and energy quality analyzers calibrated by the GEPEA-EPUSP renewable energies indoor laboratory. No issues were found during the operation tests in the generation system. Based on the voltage and current data obtained during this stage of the commissioning, it was possible to determine the proper functioning of the solar microinverters MPPT algorithms. Table 2 shows the MPPT voltage and current values, measured and estimated through the mathematical model of the PV cell, obtained on 7 June 2017, at 12:04 p.m., for the radiation values on the tilted surface of 862 W/m^2 and PV cell temperature of $59.7 \text{ }^\circ\text{C}$. More than 3.28% difference in generated, theoretical, and measured electric power is observed. This difference is within the efficiency range of the MPPT algorithms of the commercial solar inverters. The thermographic inspection of the PV modules and electric panels was also carried out on 7 June 2017. No issues were found by this inspection.

Table 2. Theoretical and measured voltage and current values on the PV modules of ODTU.

	V_{mp} [V]	I_{mp} [A]	P_{mp} [W]
Theoretical value	26.18	7.45	195.0
Measured value	26.56	7.10	188.6

2.5.3. Calibration of the DC Voltage, DC Current and AC Electric Power Sensors

Differently from the other sensors, the DC voltage and current, and AC electric power transducers were not provided with a calibration certificate. Therefore, the calibration of these sensors was made using voltmeters, ammeters and energy quality analyzers calibrated by the GEPEA-EPUSP renewable energies indoor laboratory. Due to the intermittence of the solar radiation, it was impractical to carry out the calibration of the sensors directly from the solar energy production by the PV modules. Therefore, two controllable DC voltage sources were used as “replacement” for the PV modules. It was thus possible to control the voltage and current levels applied to the entrance of the solar microinverters, and to raise the “operation curve” of each of the 06 voltage sensors, 06 current sensors and 02 electric power sensors composing the ODTU.

3. Results and Discussion

3.1. Pre-Operation of the ODTU Water-Film

The performance analysis of the ODTU electric power generation before the beginning of the cooling system operation means that, throughout this period, the cooling system is off, to understand the regular operating conditions of the PV modules, solar inverters and monitoring system. This process is important to determine the generation differences of each module, which can present differences in the outlet electric power of $\pm 5\%$, and cause an overestimated gain of the cooling system, or even underestimate its performance once the reference module can present a generation different from the cooled PV modules.

The pre-operating analysis of the ODTU consists of seven consecutive days of operation between 3 and 9 September 2017 and, for the period between 9:30 a.m. and 3:30 p.m. These consecutive days were chosen because they have a high frequency of temperature and radiation. This condition occurs because the month of September, mainly the first

fortnight, in this region presents high insolation rate, small cloud cover, low humidity, low precipitation, and average daily temperatures above 23 °C [73]. In addition, the average amount of clouds at the site decreased from sunrise until around 11 a.m., subsequently presenting a monotonic increase until sunset, when it reaches the highest cloud cover [74], positively affecting the incidence of solar radiation in the PV modules. Regarding the weather conditions, the period is between 6:00 a.m. and 6:00 p.m. On these days, the variation of the solar radiation on the tilted surface of the modules [W/m^2] and the ambient temperature [$^{\circ}\text{C}$] varied, with the highest levels for both parameters happening at noon (see Figure 3). The daily maximum values overlap, reaching values over $1000 \text{ W}/\text{m}^2$ and $28.0 \text{ }^{\circ}\text{C}$. Regarding the daily averages, the solar radiation varies between 792.7 and $892.7 \text{ W}/\text{m}^2$, and the ambient temperature is $26.4 \text{ }^{\circ}\text{C}$.

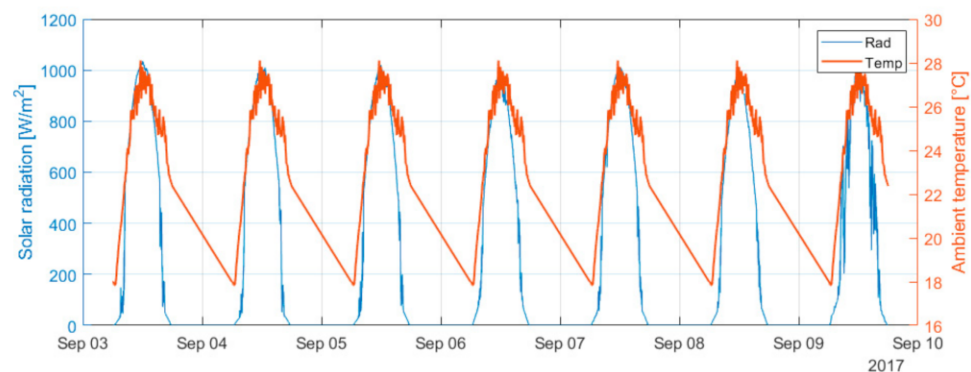
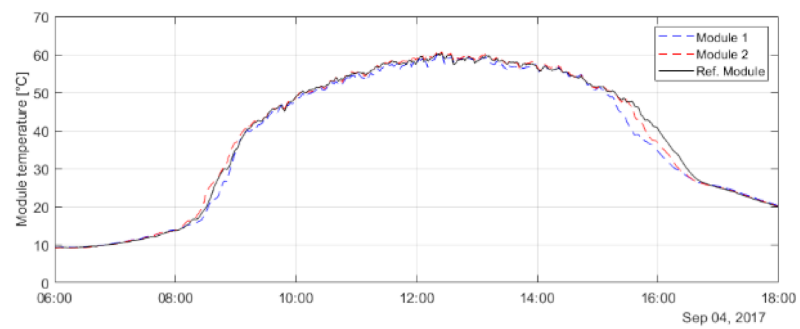


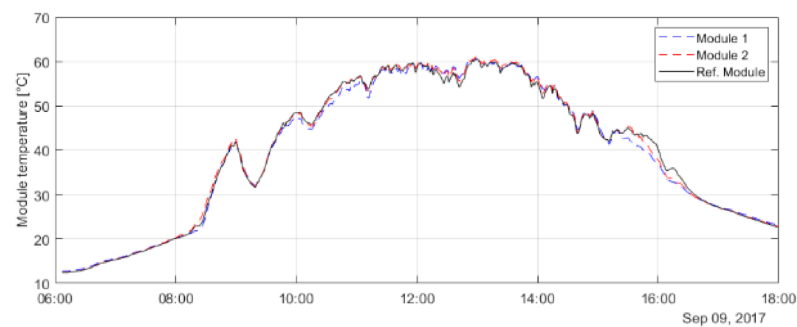
Figure 3. Variation of solar radiation and ambient temperature.

While high levels of solar radiations are beneficial for electric power production by the PV modules, these environmental conditions increase the operating temperature of the PV modules. The temperatures vary throughout the day, with the highest temperatures occurring between 11:00 a.m. and 2:00 p.m., reaching levels over $60 \text{ }^{\circ}\text{C}$ —a value found in the international literature [12,20,37,75,76] and involves the worsening of the degradation of the solar cells causing significant energy yield losses (kWh) [77]—in some periods (see Figure 4). The three modules—PV1, PV2, and PV4—present a small difference in temperature, once the temperature lines do not overlap. Regarding their averages, the difference between PV1 and PV2 in comparison to PV4 is lower at $1.0 \text{ }^{\circ}\text{C}$. It can be observed that PV2 presents a slightly higher temperature than modules PV1 and PV4, although it is not recurrent in the period (see Table 3).

As occurs with the variation in temperature of the PV module throughout the day, the output electric powers of the system overlap and suffer variation with minimum values occurring at the beginning and end of the day, and maximum values between 11 a.m. and 2 p.m. at levels above 200 W (see Figure 5). It is evident that PV4 has a better performance than PV1 and PV2, with average and maximum electric powers of 186.56 and 220.59 W , followed by PV2, with 184.17 and 220.25 W , and the PV1, with 178.29 and 219.18 W . Regarding electric power generation, PV1 and PV2 and PV4 generate 7.79 , 7.74 and 7.84 kWh/week , respectively. As expected, PV4 presents the highest yield among the modules, as it is 4.43% higher than PV1, and 1.28% higher than PV2 (see Table 4). These numbers show that PV1 and PV2 present lower performance than PV4, which is an important finding, once the cooling system will incisively act on PV1 and PV2, that is, the yield gain from cooling will be positive, in case it surpasses the natural performance of PV4. Another important point is that the generation of gross energy of the systems is the same as the net energy, once there is no cooling system operating and, thus, there is no energy used with pumping.



(a)



(b)

Figure 4. Temperature of PV1 and PV2 (with cooling system off) and PV4 (a) 4 September 2017; (b) 9 September 2017.

Table 3. Daily average temperature of PV1 and PV2 (with cooling system off) and PV4, for the period between 9:30 a.m. and 3:30 p.m.

Day	PV1 [°C]	PV2 [°C]	PV4 [°C]	PV1/PV4 [%]	PV2/PV4 [%]
3 September 2017	52.30	52.58	52.02	100.54	101.07
4 September 2017	54.11	54.96	54.78	98.77	100.33
5 September 2017	53.66	54.94	54.95	97.65	99.98
6 September 2017	50.05	49.60	49.22	101.68	100.77
7 September 2017	52.60	52.3	51.74	101.66	101.07
8 September 2017	53.35	53.63	53.26	100.17	100.69
9 September 2017	52.88	53.32	53.04	99.69	100.52

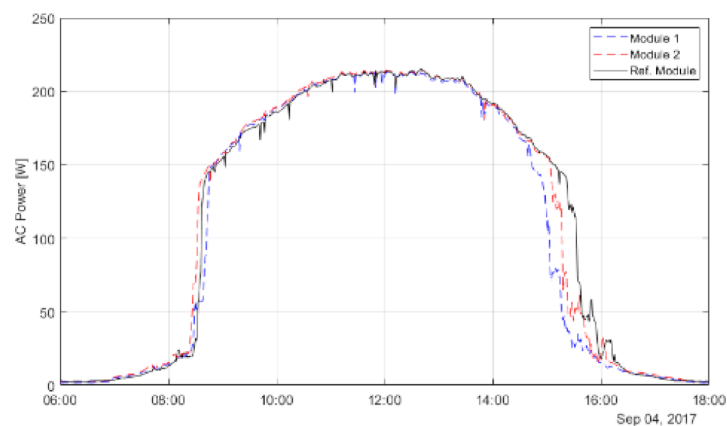


Figure 5. Output electric power of PV1 and PV2 (with cooling system off) and PV4 throughout the day 4 September 2017.

Table 4. Generation of gross AC energy and electric power between 9:30 a.m. and 3:30 p.m.

Parameter	PV1 Module	PV2 Module	PV4 Module
Total energy [kWh/week]	7.49	7.74	7.84
Average energy [kWh/day]	1.07	1.11	1.12
Maximum electric power [W]	219.18	220.25	220.59
Average electric power [W]	178.29	184.17	186.56
Total energy [%/Mod. PV4]	95.57	98.72	100
Average electric power [%/Mod. PV4]	95.57	98.72	100

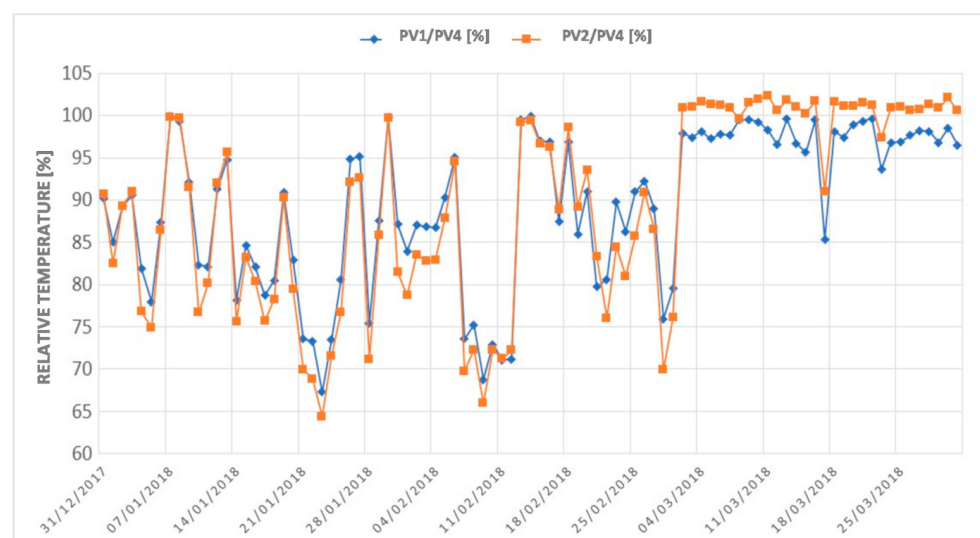
3.2. Operation of the ODTU Water-Film

The energy performance analyses of the PV modules with the water-film cooling system operating consists of the days between 31 December 2017 and 4 August 2018, see Table 5, and the period between 9:30 a.m. and 3:30 p.m., when there is no shading on the PV modules of the ODTU at this time of the year. Note that the pump used in the cooling system is oversized to meet the requirements of the research conducted at ODTU; its energy consumption was not computed for calculating the net power generation gain of the PV modules.

Table 5. Period of analysis of the functioning of the water-film.

Month	Period	Average Daily Temperature [°C]
01	31 December 2017–27 January 2018	
02	28 January 2018–24 February 2018	17–28
03	25 February 2018–31 March 2018	
04	1 April 2018–28 April 2018	
05	29 April 2018–26 May 2018	14–24
06	27 May 2018–30 June 2018	
07	1 July 2018–4 August 2018	10–28

Figure 6 shows the temperatures of PV1 and PV2 in relation to PV4 for the first quarter of the year (Summer), the average temperature reduction was approximately 18% or 8.0 °C for PV1 and PV2, with a difference of less than 2 °C in the daily average. This result was expected due to the flow sequence and consequent heating of the coolant. In this period, the average minimum and maximum daily temperatures were between 17–28 °C, see Table 5. The highest temperatures for the analyzed period were above 60 °C.

**Figure 6.** Relative temperature of the cooled modules in comparison to the reference module.

The best performance of the system from the point of view of reducing the temperature was verified on 23 January 2018, with a reduction of about 35% (21 °C). On the week between 21 January 2018 and 28 January 2018, the behavior found in the pre-operation period, in which there is a variation in the solar radiation on the tilted surface of the modules, and the ambient temperature throughout the days, with the highest values for both parameters occurring at noon (see Figure 7), the daily maximum values overlap, reaching levels over 1200 W/m² and 33.0 °C. Regarding the daily averages, the solar radiation varies between 407–803 W/m², and the average ambient temperature varies between 23–32 °C. In this period, the average and maximum temperatures were higher than the previous period, which is a result of the change of the season of the year: in the first period, it was spring and, in the second one, it was summer. The solar radiation averages on the tilted surface of the second period are lower than the first one, even with maximum values up to 200 W/m² higher than the first period. This happens because of the longer period of cloud cover and rains on the site.

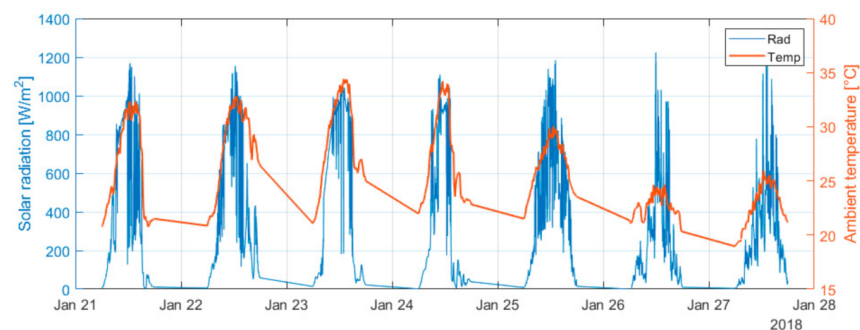


Figure 7. Variation of solar radiation [W/m²] and ambient temperature [°C].

Figure 8 presents the temperature of PV1 and PV2 and PV4 on the days with the highest and lowest solar radiation average on the tilted surface. On these days, the operation of the cooling system greatly reduces the temperature of the PV1 and PV2, which reach temperatures of 40 °C, while PV4 operates above 65 °C—higher than the Pre-operation period; a 25 °C difference (see Figure 8a). On a day with low rates of solar radiation, PV1 and PV2, in comparison to PV4, have little difference in temperature; in some periods, the temperature is the same (see Figure 8b).

The difference in daily average temperatures of PV1 and PV2, in comparison to PV4, reach 32.7% and 35.6%, respectively, on 23 January 2018, showing that the cooling system greatly reduces the temperature of the modules. The difference in temperature between PV1 and PV2 is subtle—less than 2.0 °C on the daily average, lower than systems by closed-circuit cooling system (>2 °C) [12,78]. This result is expected, due to the following flow and consequent heating of the fluid. The maximum drop in operating temperature of the cooled modules occurred on 23 January 2018, with a 35.6% reduction—or −21 °C—in comparison to PV4.

The difference in average temperature of the inlet and outlet water of the cooling system is over 6.0 °C for some days of the analyzed period. On 23 January 2018, the day with the longest period of pump operation (262 min/day), when it had to be started the most (25 times), and had the highest energy consumption (855.9 Wh/day), the difference in mean temperature between inlet and outlet is 3.2 °C. This is the smallest difference registered in the period, caused by the highest daily mean temperature of the 1.0 m³ tank, which heats throughout the day during the operation of the cooling system (see Table 6).

Figure 9 shows that on the days when the water-film was not operating, energy generation in PV1 and PV2 was naturally lower than the generation in module PV4, as presented in the operating period of the ODTU with the cooling system off. PV1 and PV2 present a 2.6% and 2.1% decrease in generation, respectively, in comparison to PV4, during the days when the water-film is not operating.

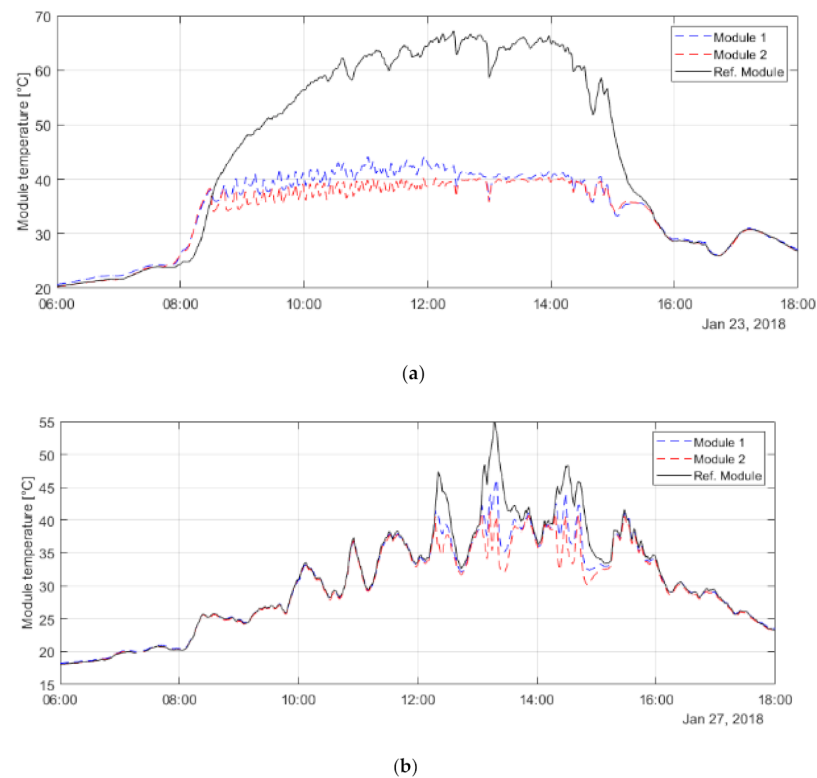


Figure 8. Temperature of PV1 and PV2 and PV4 (a) 23 January 2018; (b) 27 January 2018.

Table 6. Data measured from pump and water operation (2018).

Day	Energy [Wh/day]	Operation [min/day]	No. of Starts	Average Flow [L/min]	Average Inlet Water Temp. [°C]	Average Outlet Water Temp. [°C]	Average Water Temp. 1.0 m ³ Tank [°C]
21 January 2018	277.27	145	40	2.42	31.80	36.81	28.24
22 January 2018	322.22	160	37	2.45	31.64	37.22	28.35
23 January 2018	855.86	262	25	3.18	34.22	37.38	30.74
24 January 2018	553.14	177	15	3.08	34.28	37.50	30.87
25 January 2018	173.98	105	35	2.54	31.86	35.37	29.32
26 January 2018	25.13	19	7	1.96	27.71	31.77	26.26
27 January 2018	22.29	19	7	2.23	26.64	32.48	24.15

When the cooling system is operating intensively, it can be observed that the PV1 and PV2 generate, on average, 3.4% and 1.9% of the energy of PV4, respectively. Compensating the natural generation deficit of the cooled modules, it can be estimated that the water-film increases the generation of PV1 and PV2, on average, by 6% and 4%, respectively. Even though the operating temperatures of PV2 is lower than that of PV1, the gain obtained in PV2 is lower than in module PV1. This is caused by the degradation observed in the glass of module PV2 during the operating period of the cooling system, the continuous operation of the water-film was observed to cause incrustation of a thin white crust on the top surface of the module, causing a 2.5% decrease in the performance of PV2.

The maximum gain in energy generation of PV1 and PV2 in relation to PV4 in this period occurred on 23 January 2018, when 9.3% and 8.1% more energy were generated by PV1 and PV2, respectively. This compensated the natural generation deficit in the cooled modules and ensured performance peaks of 12% and 10% for PV1 and PV2, respectively.

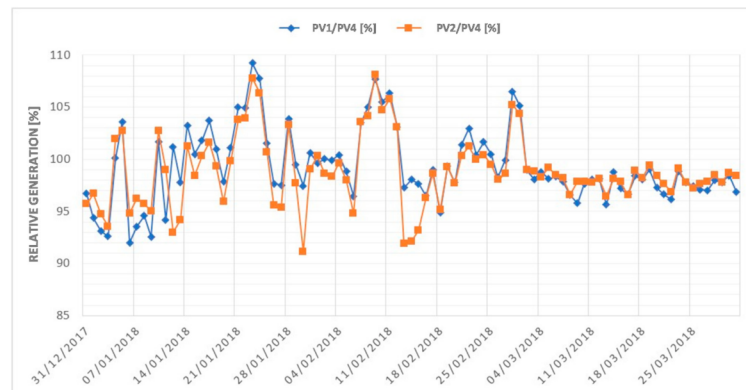
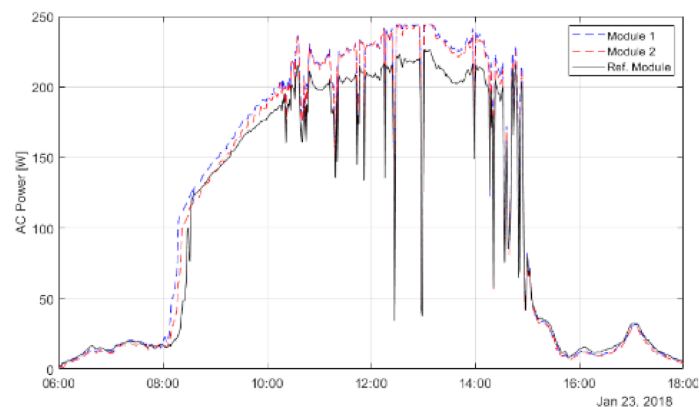
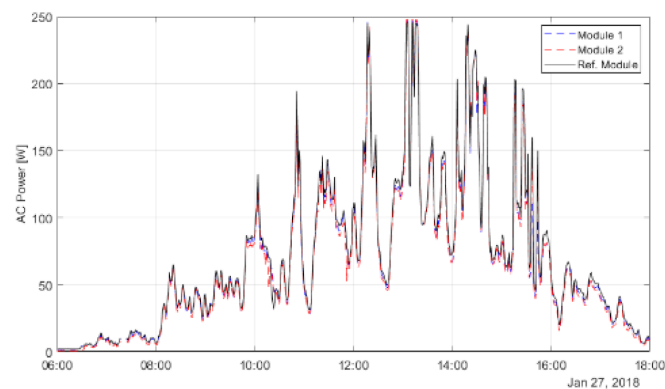


Figure 9. Gross AC energy of the cooled PV modules in comparison to the reference module.

The electric power profile linked to PV1 and PV2 and PV4, as well as the one presented previously, suffers variation, with minimum values at the beginning and end of the day, and maximum values between 11:00 a.m. and 2:00 p.m., and in levels over 200 W (Figure 10). On the days when the cooling system is operating, the outlet electric power of PV1 and PV2 is about 4.0% and 2.6% higher than PV4, respectively. Even though module PV2 is cooled before module PV1, it presents lower average electric power in 1.9 W, reinforcing that module PV2 presents a naturally lower performance than module PV1. There is a small difference between the maximum electric powers obtained by the three modules; however, the average electric power of the cooled modules is higher by more than 10.0 W.



(a)



(b)

Figure 10. Outlet electric power of PV1 and PV2 and PV4 (a) 23 January 2018; (b) 27 January 2018.

The best weekly performance, in terms of energy, was seen in the week between 21 January 2018 and 27 January 2018, with an average gain of 6% (Figure 11a,b).

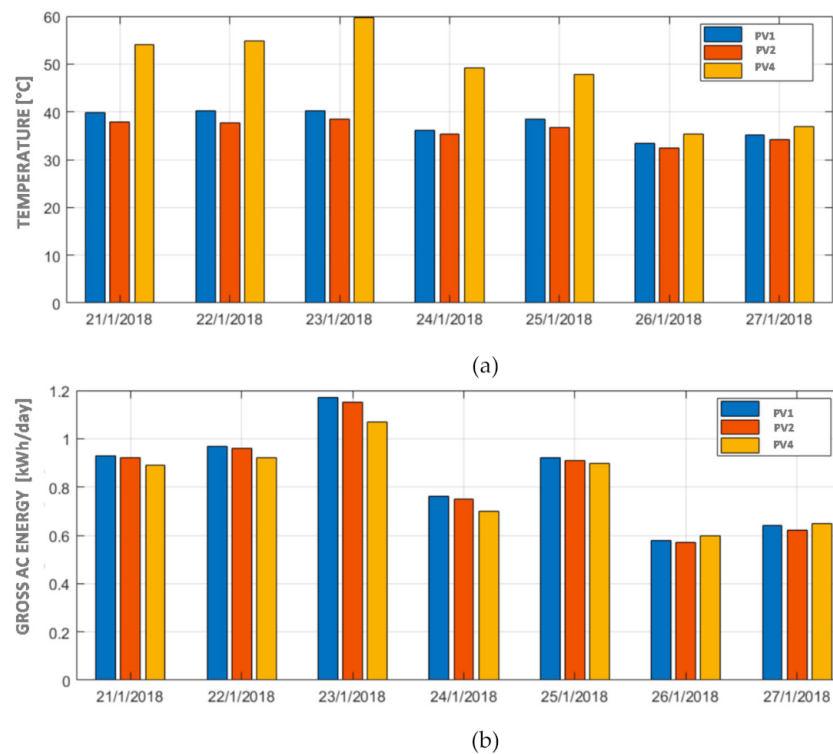


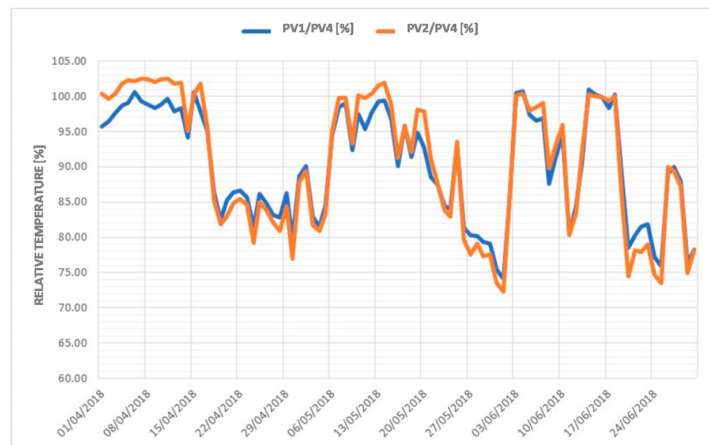
Figure 11. Week between 21 January 2018 and 27 January 2018 (a): PV temperature (b): Gross AC energy.

Considering the second quarter (autumn), the average temperature reduction was approximately 15% (7 °C) for PV1 and PV2, with a difference of less than 2 °C in the daily average. The best performance was verified on 6 January 2018, with a reduction of about 27% (13 °C), see Figure 12a. However, it is lower than that recorded in the first quarter, mainly due to the lower ambient temperatures that were in the range of 10–24 °C, see Table 5.

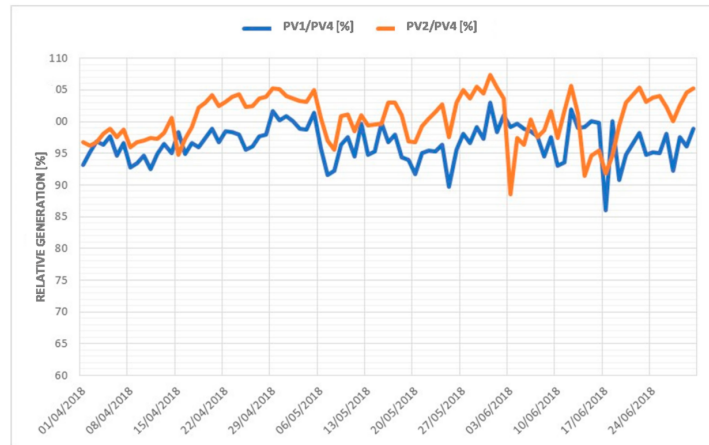
In the period of greatest solar radiation, the power gains of PV1 and PV2 in relation to PV4 were about 3% and 7%, respectively. On days with ambient temperatures above the average, for the period, the gains were 8–12% for PV1 and PV2. Such power gains reflect the increase in generation, which in the second quarter had an average increase of 3% and 5% for PV1 and PV2, with a maximum gain of 8.0% and 10.4%, recorded on 31 May 2018, for PV1 and PV2, see Figure 12b.

The best weekly performance of the second quarter, in terms of generation, was seen in the week between 29 April 2018 and 5 May 2018, in which the daily average temperatures of PV1 and PV2 were lower than that of PV4, see Figure 13a, which is also an indication that the water slide operated every day, as confirmed by flow measurements. As a result, the gross energy generated by PV1 and PV2 was always greater than or equal to that of PV4, see Figure 13b.

Analyzing the last test period (winter), July 2018, the average temperature reduction was approximately 19% (9 °C) for PV1 and PV2, with a difference of less than 0.6 °C in the daily average. The best performance being verified on 28 July 2018, with a reduction of about 31% (15.5 °C), see Figure 14a. However, it is lower than that recorded in the first quarter, mainly due to the lower ambient temperatures that were in the range of 10–28 °C, see Table 5.

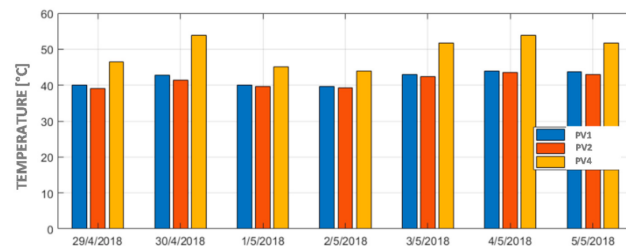


(a)

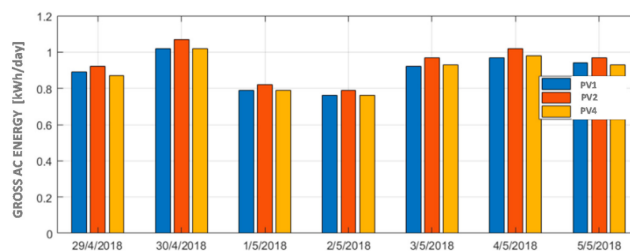


(b)

Figure 12. Second quarter of the year (a): Relative temperature of the cooled PV modules in comparison to the reference module. (b): Gross AC energy of the cooled PV modules in comparison to the reference module.

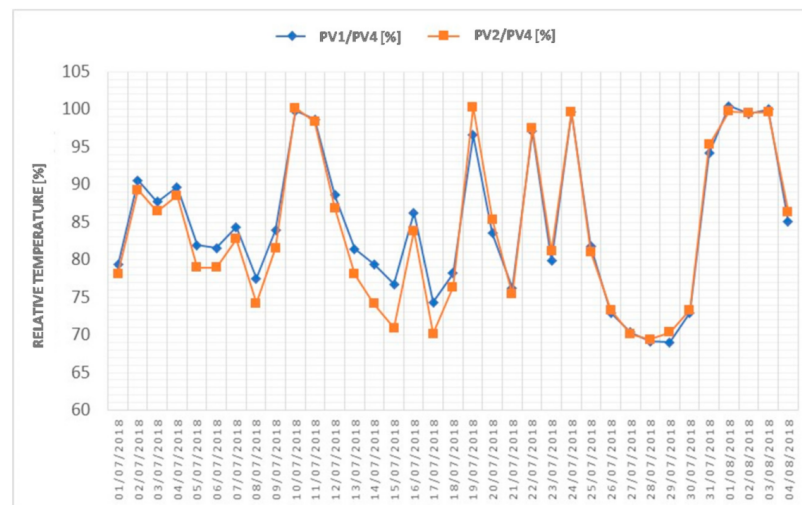


(a)

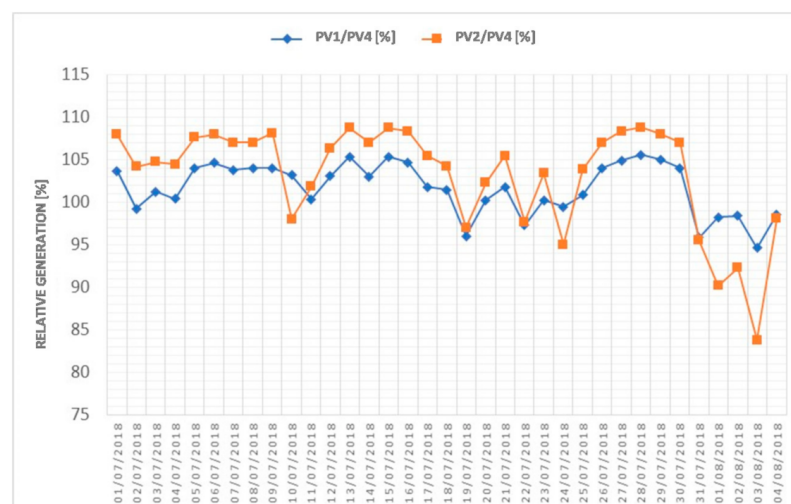


(b)

Figure 13. Week between 29 April 2018 and 5 May 2018 (a): PV temperature (b): Gross AC energy.



(a)



(b)

Figure 14. Second quarter of the year (a): Relative temperature of the PV modules in comparison to the reference module. (b): Gross AC energy of the cooled PV modules in comparison to the reference module.

As in the last two periods, in the period of greatest solar radiation, the power gains of PV1 and PV2 in relation to PV4 were about 4% and 9%, respectively. Such power gains reflect the increase in generation, which had an average increase of 1.5% and 5.2% for PV1 and PV2, with a maximum gain of 12%, recorded on 28 July 2018, for PV2, see Figure 14b. In addition, all the weekly averages of generation of the cooled PV modules were above the reference PV module, with an average weekly gain of 2% and 4%. There is a significant difference between the generation of PV1 and PV2, which did not occur in the first and second quarters of 2018. This is due to the partial degradation of the upper surface of PV1, observed only in this module in the period under study. The water on its surface was observed to take longer to evaporate after the end of the water circulation.

The best weekly performance of the last test period was observed in the week between 8 July 2018 and 14 July 2018, when the average temperatures of PV1 and PV2 on most of the days were lower than that of PV4, see Figure 15a. As a result, except for two days, the gross energy generated by PV1 and PV2 was greater than PV4, see Figure 15b.

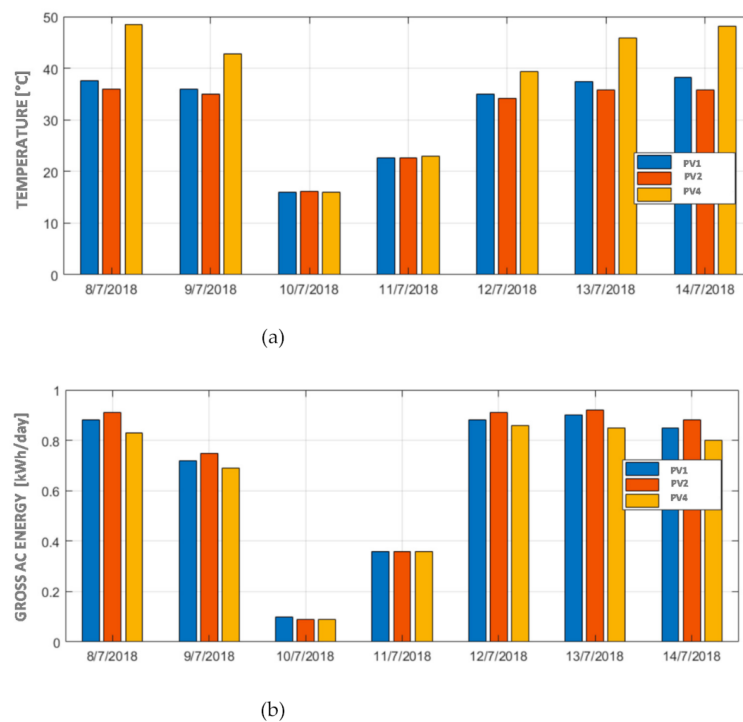


Figure 15. Week between 8 July 2018 and 14 July 2018 (a): PV temperature (b): Gross AC energy.

4. Comparative Analysis

Analyzing the literature review and comparing it with the results obtained in this work, it is possible to verify that the period of analysis was longer than other works. Empirical tests took place over three seasons (summer, autumn and winter) for low latitude and hot climates, see Table 3. On average the empirical tests found in the literature are a few days, usually one or two days, see Table A1. In addition, even in winter, the cooling system improves the net efficiency of power generation.

Comparing ODTU results with the systems presented in Tables A1 and A2, we can demonstrate that:

- It is evident that cooling systems increase the power generation of the PV modules;
- Most of the systems analyzed are in the northern hemisphere and mainly concentrated in Asia;
- In general, the average annual temperature of these locations is above 20 °C;
- Warm condition locations present the highest performance gains in power generation, while presenting the greatest reductions in the operating temperature of the PV modules when using a cooling system;
- Open cooling systems perform better than closed cooling systems;
- Except for this work and [31], all the cooling systems analyzed with more than a month of testing period are of the closed type.
- ODTU tests showed a longer execution time and better performance evaluation than the works analyzed in the literature review and systematized in Tables A1 and A2. In the case of [31,79,80], with three months of testing period with cooling system operating. However, there was no comprehensive presentation of the results over the period. The results are concentrated on specific days when the performance indexes of the PV modules were higher.
- Due to the short testing period linked to open cooling systems, it was not possible to compare the possible degradations that can occur in the PV module due to the direct contact of the water with its surface;
- During the summer, the cooling system reduced the temperature by 15–19% on average, with a maximum of 35%; this is similar to the values found in [51], tested in the

summer in a place with a cold semi-arid climate and an average annual temperature of 17.4 °C, and [81], tested in the spring in a place with hot semi-arid climate and average annual temperature of 25.2 °C;

- Regarding the gross generation, the average gains during the summer were of 2.3–6%, with maximum gains of 12%, as in [25], with a gain of 6.9% tested in the summer in a place with hot-summer-Mediterranean climate and average annual temperature of 16.1 °C, and [47], with a gain of 7.4% tested in the summer in a place with humid-subtropical climate and average annual temperature of 22 °C.
- During the winter, the average temperature reduction was approximately 19%, with a maximum reduction of about 31%. Only two other works were tested during that season. Ref. [6] with maximum reduction of 43.1% in a place with tropical savanna climate and average annual temperature of 23.5 °C, and [79], in a place with tropical rainforest climate and average annual temperature of 27.1 °C, did not simultaneously compare a cooled and an uncooled PV module.

5. Conclusions

The ODTU made it possible to carry out experiments, several measurements, and data analyses, and to visualize and to understand the operation of the water-film cooling system. The experiments allowed observing that the cooling system promotes temperature reduction of the PV modules with a consequent increase in electric power and, hence, higher energy generation. Therefore, this technique was observed to improve the energy performance of the commercial PV modules.

The water-film cooling system produced a significant decrease in the temperature of the cooled modules, with 15–19% average reduction, and 24–35% maximum reduction. In terms of electric power, the cooling system promoted 5–9% average gains in the periods with higher solar radiation, and 12% maximum gains on days with solar radiation above average. Regarding gross energy generation, a 2.3–6.0% average gain and a 6.3–12.0% maximum gain were obtained. It can be concluded that ODTU assists in: (i) understanding the natural phenomena that cause an impact on energy generation in commercial PV modules with and without a cooling system; (ii) developing a cooling system to increase the performance of PV modules, and identifying and assessing the processes and stages of operation and maintenance of this type of system for further construction and implementation, even on a commercial scale.

Over the six months of operation of the water-film, it was found that the temperature of the modules and generation vary with environmental conditions. In the summer, with high average daily temperatures, the effect of reducing the temperature of the cooled PV modules was higher than in autumn and winter months. Even in the latter two seasons, in which the average daily temperatures were between 10–28 °C, there was a gain in energy generation. This evidenced that cooling systems for PV modules in warm conditions increase energy generation, even in winter periods when temperatures are mild, as demonstrated in the work.

Another finding was that the PV module showed degradation over time, possibly caused by the late effect of water evaporation on its surface. This degradation has substantially reduced the energy generation performance of the PV module. Therefore, in cases in which an open cooling system at the top side of PV module are used, it is important to analyze the quality of the water and the effects of its use over the long term.

Author Contributions: Conceptualization, V.S., J.M. and J.B.; methodology, V.S., J.M. and R.H.; software, V.S. and J.M.; validation, V.S., J.M., R.H. and J.B.; formal analysis, V.S., J.M., R.H. and J.B.; investigation, V.S., J.M., A.G. and M.U.; resources, A.G. and M.S.; data curation, V.S., J.M., R.H. and J.B.; writing—original draft preparation, V.S. and J.M.; writing—review and editing, V.S., J.M. and M.U.; supervision, A.G., M.U. and M.S.; project administration, A.G. and M.S.; funding acquisition, A.G. and M.S. All authors have read and agreed to the published version of the manuscript.

Funding: This work was partially financed by Coordenação de Aperfeiçoamento de Pessoal de Nível Superior—Brasil (Coordination for the Improvement of Higher Education Personnel—CAPES). To

CNPQ (Conselho Nacional de Desenvolvimento Científico e Tecnológico—Brazilian National Council for Scientific and Technological Development), for the scholarship. To ITASA/ANEEL, for funding the P&D ANEEL—PD-0452-0001/2016.

Institutional Review Board Statement: Not applicable.

Informed Consent Statement: Not applicable.

Data Availability Statement: Not applicable.

Acknowledgments: To Diego Biaseto Bernhard great engineer and specialist in energy and thermal systems and the team of researchers and collaborators of the GEPEA/EPUSP, that directly and indirectly contributed to the accomplishment. To the editor and the three anonymous reviewers whose comments helped to strengthen this work.

Conflicts of Interest: The authors declare no conflict of interest.

Appendix A

Table A1. Consolidation of the characteristic of the theoretical and experimental research.

Ref/ Year	Local (City/Country)	Köppen Climate [80]	Season	Average Annual Temperature (°C)	N° PV Modules	Tilt Angle	Cooling System	Fluid	Pump	Flow Rate	Fluid Temperature (°C)	Test Period
[51] 2009	Zarqa Jordan	Cold semi-arid (BSk)	Summer	17.4	01 PV Cooled or uncooled	32°	Open system Top side of PV	Water	Submersible pump	4 L/min	Inlet: ~25	1
[81] 2011	Chuncheon Korea	Hot humid continental (Dwa)	Spring	10.9	02 PV 01 cooled 01 uncooled	23°	Open system Top side of PV	Water	Pump	10 L/min		03 days 13–15 May 2010
[48] 2011	Cambridge USA	Humid continental (Dfa)	Autumn	9.7	01 cooled	-	Close system Bottom side of PV	Water	Pump 17W	-	Inlet vs. outlet: ~4	01 day Mid-November
[24] 2013	Cairo Egypt	Hot desert (BWh)	Summer	21.3	14 PV 06 cooled 08 uncooled	-	Open system Top side of PV	Water	Pump 746 W.	29 L/min	Assumed: 25	02 days One in June and one in July 2012
[31] 2014	Portland USA	Warm-summer Mediterranean climate (Csb)	Spring and Summer	11.9	08 PV 01 cooled 07 uncooled	30°	Open system Top side of PV	Water	Pump 7W	7 L/min	With Ice: Inlet 8	03 months April to June, 2012
[82] 2014	Wysall UK	Oceanic (Cfb)	Summer	9.6	84 PV cooled	10°	Close system Bottom side of PV	Water	Pump	0.017 kg/s	-	01 day 19th July
[6] 2015	Ilha Solteira Brazil	Tropical savanna (Aw)	Winter	23.5	88 PV 44 cooled 44 uncooled	23°	Close system Bottom side of PV	Water	No pump potential energy	1.5–3 L/s	-	14 days
[49] 2015	Alexandria Egypt	Hot desert (BWh)	Spring	20.6	03 PV 01 cooled 02 uncooled	30°	Open system Top side of PV	Water	Pump	1.2 L/h	-	01 day of April 2014
[53] 2015	Perlis Malaysia	Tropical monsoon (Am)	Spring	27.3	02 PV 02 cooled or uncooled	-	Open system Top and Bottom side of PV	Water and air	Pump	-	-	01 day 31 March 2014
[52] 2015	Kerman Iran	Cold desert (BWk)	Summer	16	03 cooled	30°	Open system Top side of PV	Water	Pump	-	-	03 days June and July
[20] 2016	Abu Dhabi UAE	Hot desert (BWh)	1	26.8	01 cooled	60°	Close system Bottom side of PV	Water	Pump	0.063 kg/s	Inlet: 30	01 month
[25] 2016	Split Croatia	Hot-summer Mediterranean (Csa)	Summer	16.1	01 cooled	17°	Open system Top and Bottom side of PV	Water	Pump 4.2 W	225 L/h	Inlet: 17	01 day

Table A1. Cont.

Ref/ Year	Local (City/Country)	Köppen Climate [80]	Season	Average Annual Temperature (°C)	N° PV Modules	Tilt Angle	Cooling System	Fluid	Pump	Flow Rate	Fluid Temperature (°C)	Test Period
[83] 2017	São Paulo Brazil	Oceanic (Cfb)	Summer and Autumn	18.5	05 PV 02 cooled 03 uncooled	23°	Close system Bottom side of PV	Water	Pump	0.07–0.48 L/s	Inlet: 20.5–21.5	11 months (03 months with cooling system)
[84] 2017	Kuala Lumpur Malaysia	Tropical rainforest (Af)	Winter	27.1	01 cooled	0°	Close system Bottom side of PV	Water	Pump	30–180 L/h	-	03 months January to March 2015
[12] 2018	São Paulo Brazil	Oceanic (Cfb)	Summer	18.5	05 PV 02 cooled 03 uncooled	23°	Close system Bottom side of PV	Water	Pump	-	-	21 days
[22] 2018	Kuala Lumpur Malaysia	Tropical rainforest (Af)	Winter	27.1	01 cooled	0°	Close system Bottom side of PV	Water	Pump	30–180 L/h	Inlet: 30	01 months February
[44] 2018	Lodz Poland	Warm humid continental (Dfb)	Autumn	6.7	02 cooled	30°	Close system Bottom side of PV	Water	Solar Pump	1.3 kg/min	-	01 day 01 October 2015
[46] 2018	Hefei China	Humid subtropical (Cfa)	Summer	16	03 PV 02 cooled 01 uncooled	32°	Close system Bottom side of PV	Water	Pump	0.06 L/s	-	June and July 2017
[47] 2018	Taiwan China	Humid subtropical (Cfa)	Summer	22	01 cooled	23.5°	Open system Bottom side of PV	Water	Pump	0.57 L/min	-	Maybe July
[54] 2018	Catania Italy	Hot-summer Mediterranean (Csa)	Spring	17.8	02 cooled	25°	Close system Bottom side of PV	Water	Pump 3–45 W	55 L/min	-	07 days 3 to 9 May 2017
[79] 2018	New Delhi India	Hot semi-arid (BSh)	Spring	25.2	05 cooled	28°	Open system Top side of PV	Water	1	-	-	02 days April 2017
[85] 2019	Bucaramanga Colombia	Tropical rainforest (Af)	1	23.4	10 PV 03 cooled 07 uncooled		Open system Top side of PV	Water	Submergible pump	1.75 L/min 3.75 L/min 4.75 L/min 9.50 L/min	-	1
[86] 2019	Elche Spain	Cold semi-arid (BSk)	Summer	17.8	02 PV 01 cooled 01 uncooled	45°	Open system Top and Bottom side of PV	Water	Pump	0–80 L/h	-	01 day July 26. 2016

¹ Not specified.

Table A2. Consolidation of the results of the theoretical and experimental research.

Ref/ Year	Theoretical Research	Experimental Research	Thermal Results	Electric Results
[51] 2009	Thermoelectric model for hourly solar radiation data for different locations in Australia:	Test of system performance under different radiation conditions, but does not compare the cooled with uncooled PV module at the same time	PV temperature (°C): Uncooled: ~58 Cooled: decreases about 26	The increase in cell temperature above the standard operating temperature (45 °C) caused a drop of 5% in output power. Power gain with cooling system: about 15%
[81] 2011	Thermal model of the surface cooling system	Compare and validate the thermal model results with the results of the empirical tests. Compare the cooled with uncooled PV module	PV temperature: Deviation between measured and predicted model is <4 °C. Maximum deviation between the cooled and uncooled was 20 °C	Average voltage gains with cooling system were 1.2/2.2/1.4 V for each test day. Maximum voltage gain was 3.2 V. Maximum power gain with cooling system was 11.6%
[48] 2011	Thermal model to determine the production of clean water based on the increase of the cooling water temperature of the PV modules	Compare the measured with the predicted model. Determine the PV temperature with and without cooling system, but does not compare the cooled with uncooled PV module	PV temperature: Cooled: decreases by 10 °C With thermal management, additional gain of about 10 °C	With thermal management there is a gain of about 50 W
[24] 2013	Thermal model to determine how long it will take to cool the PV modules to the normal operating temperature minimizing the amount of water and energy needed for cooling	Determine the influence of cooling and overheating on the performance of the PV cells, but does not compare the cooled with uncooled PV module at the same time	PV temperature: Simulated 46 and measured 42.5. Temperature reduction of 10 °C after the cooling system has operated for 5 min	Theoretical: The output power is 790 W for 35 °C and 640 W for 65 °C. Experimental: determines that the efficiency of operating at 45 °C is 10.5% and for 35 °C, 12.5%
[31] 2014	-	Explored various applications of the surface water cooling system: (i) open rack modules; (ii) insulated PV modules, (iii) ice water in the cooling system; and (iv) combining cooling system with concentrating methods	PV temperature (°C): (i) cooled 20–35/uncooled 40–60 (ii) cooled 20–40/uncooled 20–50 (iii) cooled 20–35/uncooled 20–55 (iv) cooled 20–40/uncooled 40–55	(i) 12% average energy gain; after accounting for pump power consumption, 6%; the total power output gain over the course of the day was 9.4% and the total net energy gain was 4.6% (ii) gain in relation to the isolated modules was 14%, discounting the pumping energy, the net energy gain was 8.3% (iii) the inlet water temperature was 8 °C, minimum module temperature 16 °C, with instantaneous power gain of 24% (iv) it reached the maximum power of the inverter; it was not possible to determine the gain of both systems operating on the module, reaching 200W, with a power gain of 43%
[82] 2014	Thermal model to determine conversion of solar radiation into thermal energy by PV module absorbers and transporting absorbed thermal energy towards polyethylene heat exchangers	Examine the effectiveness of a cooling system in the improvement of the PV cell efficiency and compare the measured with the predicted model cumulative water produced	PV temperature: Experimental values indicate that water temperature difference could reach up to 16 °C. Simulated 62 °C and measured 57 °C	-
[6] 2015	-	Determine the increase in electrical performance of a PV plant with cooling system and compare the cooled with uncooled PV module	PV temperature (°C): uncooled 60 cooled 34.1	Maximum power gain was 6.5% Daily generation gain of 5.9%

Table A2. Cont.

Ref/ Year	Theoretical Research	Experimental Research	Thermal Results	Electric Results
[49] 2015	-	Explore the automatic cooling and cleaning system in the performance of PV modules and compare the cooled with uncooled PV module	PV temperature (°C): Top side: uncooled 44/cooled 24. Bottom side: uncooled 51/cooled 31	Maximum power: cooled 89.4 W/uncooled 68.4 W. Power gain 26% Efficiency: cooled 11.7%/uncooled 9%
[53] 2015	-	Compare two open systems: 01 DC brushless fan at the bottom side of the PV module 01 DC water pump with inlet/outlet manifold at the top side of the PV module Compare the cooled with uncooled PV module	PV temperature (°C): Water pump: cooled 37.6 °C/uncooled 45.7 °C. The temperature variation of the PV module without a cooling system increased 6.4 °C with and without DC brushless fan. The average temperature of PV module along with the cooling system can be 44.8 °C, while the average temperature of PV without a cooling system seems to be 50.9 °C. The temperature variant of the PV module without a cooling system seemed to rise 6.1 °C reviews.	Gain of output voltage/output current/output power: Water pump: 3.5%/36.3%/39% Brushless fan: 3.5%/29.6%/32.2%
[52] 2015	-	Investigate how the booster reflector and water film over the PV modules affect their performance. Compare the cooled with uncooled PV module	PV temperature/Maximum temperature: (i) without reflector 59 °C/65 °C; (ii) with water film 36 °C/41 °C; (iii) with reflector 71 °C/84 °C; (iv) with reflector and water film simultaneously 39 °C/48 °C	Mean Daily Power: (i) without reflector 51.6W; (ii) with reflector 58.8 W; (iii) with water film 60.8 W; (iv) reflector and water film 77.6 W Power gain in relation to a conventional module: (i) -; (ii) 14%; (iii) 17.8%; (iv) 50.4%
[20] 2016	Thermoelectric model to determine the PVT module transient temperature and the to increase the overall PV effectiveness	Analyze the performance of each series-connected PV cell in PVT modules. Compare and validate the measured with the predicted model	PV temperature: Difference between the measured and the modelled is 8–12% The measured difference between cooled and uncooled is 5–10 °C	Recommended for environments with high ambient temperature and solar radiation
[25] 2016	Thermal model to evaluate the energy efficiency	Analyze the cooling effect impact on the power output and electrical efficiency. Analyze four applied cooling options: (i) Without cooling; (ii) Back surface cooling; (iii) Top surface cooling; (iv) Simultaneous surfaces cooling	Average PV temperature: (i) 56 °C (ii) 33.7 °C (iii) 29.6 °C (iv) 24.1 °C	Maximal power output/Relative increase in power output: (i) 35 W/-; (ii) 39.9 W/14%; (iii) 40.1 W/14.6%; and (iv) 40.7 W/16.3% Electrical efficiency/Effective increase: (i) 13.9%/-; (ii) 15.6%/3.6%; (iii) 15.4%/2.5%; and (iv) 15.9/5.9%
[83] 2017	Thermal model to evaluate the energy produced	Analyze the thermal and electrical performance of two different models of cooling systems for PV modules and compare cooled and uncooled PV modules	PV temperature: Maximum 68°C uncooled and minimum at the same time cooled 42.5 °C. The measured temperature difference between cooled and uncooled PV is 25.6°C	-

Table A2. Cont.

Ref/ Year	Theoretical Research	Experimental Research	Thermal Results	Electric Results
[84] 2017	Thermal model to evaluate the energy efficiency	Investigate the effects of the PV module operating parameters on the output power and efficiency. Does not compare the cooled with uncooled PV module at the same time	-	Electrical efficiency decreases by 5.82% as the temperature increases by 26.1 °C. Electrical efficiency decreases by approximately 0.22% as the temperature increases by 1.0 °C. When the irradiation intensity increases by 100 W/m ² the temperature increases by 3.8 °C and the output power increases by 3.14 W
[12] 2018	-	Present the development, production, installation, and performance testing of three cooling system models. Compare the cooled with uncooled PV modules	Temperature reduction: average of 20.5 °C and maximum 25.6 °C	-
[22] 2018	Thermal model to evaluate the effect of high irradiation on PV power generation, due to a lens concentrator, to optimize the flow rate of the cooling fluid and thermal energy conversion	Compare and validate the measured with the predicted model. Does not compare the cooled with uncooled PV module at the same time	PV temperature: For every 100 W/m ² in solar radiation, the temperature increases about 0.9 °C The temperature difference between the measured and the modelled is 3.3–4.2%	For every 100 W/m ² increase in solar radiation the electrical power and electrical efficiency increase about 19.65 W and 0.06%, respectively. For every 10 L/h increment of fluid flow rate, the electrical efficiency increases about 0.43%
[44] 2018	Thermal model and simulation using specialized computer program	Analyze the relationship between orientation of PVT collectors and their thermal and electric power generation, but does not compare the cooled with uncooled PV module	-	The efficiency of the PV module increases with the altitude angle, both in laboratory and field experiments
[46] 2018	Experimental evaluation of the performance of two PV/T system: (i) pipe-based PV/T; (ii) PV/T with MHPA; (iii) conventional PV module at high ambient temperature.	-	The temperature could be up to (°C): (i) 90; (ii) 70; (iii) 100 Ambient temperature between 36–40 °C and solar radiation >800 W/m ²	Electrical efficiency decreased: (i) pipe-based PV/T: 9.6% to 7.7% (ii) PV/T with MHPA: 11.2% to 10% (iii) Conventional: 8.6% to 7%.
[47] 2018	A mathematical model is built for predicting the system performance	Spray water on the bottom side of the PV. The pump was switched on once the PV temperature reached 45 °C and was switched off when it cooled to 35 °C	-	Experimental (875.9 W/m ²) Average power output (W): 33.0; 37.4; 37.5 Average net power output (W): 33.0; 33.4; 35.8 Conversion efficiency (%): 6.77 6.87 7.38 Theoretical (800 W/m ²) Average power output (W): 38.8; 43.5; 44.0 Average net power output (W): 38.8; 40.6; 42.4 Conversion efficiency (%): 8.72 9.13 9.52 Efficiency increment (%): -; 4.70; 9.17

Table A2. Cont.

Ref/ Year	Theoretical Research	Experimental Research	Thermal Results	Electric Results
[54] 2018	Mathematical model is built for predicting the system performance	-	Maximum difference in the bottom side temperatures between two modules are 3.0–4.0 °C	Cooling system increased the electrical power generated by 1.5%. Average errors of 12.1% and 5.3%, respectively, for the thermal and electrical energy produced
[79] 2018	Thermal model (analytical) to evaluate the influence of temperature on the performance of building integrated photovoltaic-thermal system	Compare and validate the measured with predicted model for five technologies: (i) m-Si; (ii) p-Si; (iii) a-Si; (iv) CdTe; (v) CIGS	Maximum daily average temperature (°C): Cooled: ~36 Uncooled (i) 49.8; (ii) 50; (iii) 53; (iv) 54; (v) 58 Maximum fluctuation is observed in CIGS	Daily average electrical energy output (%): Cooled: (i) 12.3; (ii) 11; (iii) 6.1; (iv) %, 6.6; (v) 7.7 Uncooled: (i) 11.4; (ii) 10.3; (iii) 5.9; (iv) 6.3; (v) 7.0
[85] 2019	-	Experimental characterization of the operating temperature and output power from irrigated, 255 W PV modules, considered twelve irrigation regimes with four flow rates (L/min): 1.75; 3.75; 4.75; 9.50 and four operating cycles (1':29', 5':25', 15':15', and continuous.	PV continues its cooling process for 1–5 min after irrigation ends due to the evaporation of the residual water film that formed over its front surface; the temperature decreases between 0–15 °C.	Irrigation can enhance daily energy production by 10%. A flow rate equal to or greater than 3.75 L/min (2.34 L/min/m ²) produces similar effects. Generated power increase: 0.5–2% for 400 W/m ² ; 2–5% for 400–800 W/m ² ; 5–10% for 800 W/m ²
[86] 2019	-	Experimental evaluation of the improvement in efficiency of a PV module cooled by water sliding on its upper face and on its back side using a solar chimney.	The evaporative cooling efficiency has an average value of 33.9%.	The electrical efficiency: 50 L/h improvement to 6–7%; 250 L/h maintained about 10% with a peak of 11%

References

1. Grimoni, J.A.B.; Galvão, L.C.R.; Udaeta, M.E.M.; Kanayma, P.H. *Introduction to Concepts of Energy Systems for Clean Development [Iniciação a Conceitos de Sistemas Energéticos Para o Desenvolvimento Limpo]*, 2nd ed.; Edusp: São Paulo, Brazil, 2015.
2. Udaeta, M.E.M.; Galvão, L.C.R.; Rigolin, P.H.d.; Bernal, J.L.d. Full assessment energy-sources for inclusive energy-resources planning. *Renew. Sustain. Energy Rev.* **2016**, *66*, 190–206. [[CrossRef](#)]
3. Hader, M.; Al-Kouz, W. Performance of a hybrid photovoltaic/thermal system utilizing water-Al₂O₃ nanofluid and fins. *Int. J. Energy Res.* **2019**, *43*, 219–230. [[CrossRef](#)]
4. Abdullah, A.L.; Misha, S.; Tamaldin, N.; Rosli, M.A.M.; Sachit, F.A. Numerical Analysis of Solar Hybrid Photovoltaic Thermal Air Collector Simulation by ANSYS Numerical Analysis of Solar Hybrid Photovoltaic Thermal Air Collector Simulation by ANSYS. *CFD Lett.* **2019**, *11*, 1–11.
5. Oh, J.; Govinda, S.; Tamizh, M. Temperature testing and analysis of PV modules PER ANSI/UL 1703 and IEC 61730 standards. In Proceedings of the 2010 35th IEEE Photovoltaic Specialists Conference, Honolulu, HI, USA, 20–25 June 2010; pp. 984–988. [[CrossRef](#)]
6. Da Silva, V.O. *Data Analysis on Performance of PV System Installed in South and North Directions*; Universidade de São Paulo: São Paulo, Brazil, 2016. [[CrossRef](#)]
7. Aste, N.; Del Pero, C.; Leonforte, F. Water PVT Collectors Performance Comparison. *Energy Procedia* **2017**, *105*, 961–966. [[CrossRef](#)]
8. Elbreki, A.M.; Alghoul, M.A.; Al-Shamani, A.N.; Ammar, A.A.; Yegani, B.; Aboghrara, A.M.; Rusaln, M.H.; Sopian, K. The role of climatic-design-operational parameters on combined PV/T collector performance: A critical review. *Renew. Sustain. Energy Rev.* **2016**, *57*, 602–647. [[CrossRef](#)]
9. Yamaguchi, T.; Kawakami, M.; Kitano, K.; Nakagawa, S.; Tokoro, T.; Nakano, T. Data analysis on performance of PV system installed in south and north directions. In Proceedings of the 3rd World Conference on Photovoltaic Energy Conversion, Osaka, Japan, 11–18 May 2003; pp. 2239–2242.
10. Kozak, T.; Maranda, W.; Napieralski, A.; De Mey, G.; De Vos, A. Influence of Ambient Temperature on the Amount of Electric Energy Produced by Solar Modules. In Proceedings of the 2009 MIXDES-16th International Conference Mixed Design of Integrated Circuits & Systems, Lodz, Poland, 25–27 June 2009; pp. 351–354.
11. Irwanto, M.; Irwan, Y.M.; Safwati, I.; Leow, W.-Z.; Gomesh, N. Analysis Simulation of the Photovoltaic Output Performance. In Proceedings of the 2014 IEEE 8th International Power Engineering and Optimization Conference (PEOCO2014), Langkawi, Malaysia, 24–25 March 2014; pp. 477–481. [[CrossRef](#)]
12. Da Silva, V.O.; Gimenes, A.L.V.; Udaeta, M.E.M. Development of a real-scale cooling module for a PV power plant. *IET Renew. Power Gener.* **2018**, *12*, 450–455. [[CrossRef](#)]
13. Canadina Solar Inc. Quartech CS6K-270/275M: PV Module Product Datasheet V5.3 EN. 2015. Available online: www.canadiansolar.com (accessed on 10 April 2017).
14. SunEdison. *MEMC Silvantis™ P290 Modulo, Data Sheet_Q2 2012*; SunEdison: Maryland Heights, MO, USA, 2012.
15. Siecker, J.; Kusakana, K.; Numbi, B.P. A Review of Solar Photovoltaic Technologies. *Renew. Sustain. Energy Rev.* **2016**, *55*, 414–425. [[CrossRef](#)]
16. Joshi, S.S.; Dhoble, A.S. Photovoltaic -Thermal systems (PVT): Technology review and future trends. *Renew. Sustain. Energy Rev.* **2018**, *92*, 848–882. [[CrossRef](#)]
17. Li, G.; Shittu, S.; Diallo, T.M.O.; Yu, M.; Zhao, X.; Ji, J. A review of solar photovoltaic-thermoelectric hybrid system for electricity generation. *Energy* **2018**, *158*, 41–58. [[CrossRef](#)]
18. Mellor, A.; Alonso Alvarez, D.; Guarracino, I.; Ramos, A.; Riverola Lacasta, A.; Ferre Llin, L.; Murrell, A.J.; Paul, D.J.; Chemisana, D.; Markides, C.N.; et al. Roadmap for the next-generation of hybrid photovoltaic-thermal solar energy collectors. *Sol. Energy* **2018**, *174*, 386–398. [[CrossRef](#)]
19. Hasan, M.A.; Sumathy, K. Photovoltaic thermal module concepts and their performance analysis: A review. *Renew. Sustain. Energy Rev.* **2010**, *14*, 1845–1859. [[CrossRef](#)]
20. Al Tarabsheh, A.; Ghazal, A.; Asad, M.; Morci, Y.; Etier, I.; El Haj, A.; Fath, H. Performance of photovoltaic cells in photovoltaic thermal (PVT) modules. *IET Renew. Power Gener.* **2016**, *10*, 1017–1023. [[CrossRef](#)]
21. Hasanuzzaman, M.; Malek, A.B.M.A.; Islam, M.M.; Pandey, A.K.; Rahim, N.A. Global advancement of cooling technologies for PV systems: A review. *Sol. Energy* **2016**, *137*, 25–45. [[CrossRef](#)]
22. Nasrin, R.; Hasanuzzaman, M.; Rahim, N.A. Effect of high irradiation and cooling on power, energy and performance of a PVT system. *Renew. Energy* **2018**, *116*, 552–569. [[CrossRef](#)]
23. Endecon Engineering. A guide to photovoltaic (PV) system design and installation: Energy technology development division, consultant report, a guide to photovoltaic (PV) system design and installation. San Ramon, California. 2001. Available online: https://www.energy.ca.gov/reports/2001-09-04_500-01-020.PDF (accessed on 12 May 2017).
24. Moharram, K.A.; Abd-Elhady, M.S.; Kandil, H.A.; El-Sherif, H. Enhancing the performance of photovoltaic panels by water cooling. *Ain Shams Eng. J.* **2013**, *4*, 869–877. [[CrossRef](#)]
25. Nizetic, S.; Coko, D.; Yadav, A.; Grubisic-Cabo, F. Water spray cooling technique applied on a photovoltaic panel: The performance response. *Energy Convers. Manag.* **2016**, *108*, 287–296. [[CrossRef](#)]

26. Moradi, K.; Ebadian, M.A.; Lin, C.X. A review of PV/T technologies: Effects of control parameters. *Int. J. Heat Mass Transf.* **2013**, *64*, 483–500. [[CrossRef](#)]
27. Abdullah, A.L.; Misha, S.; Tamaldin, N.; Rosli, M.A.M.; Sachit, F.A. Photovoltaic thermal /solar (PVT) collector (PVT) system based on fluid absorber design: A review. *J. Adv. Res. Fluid Mech. Therm. Sci.* **2018**, *48*, 196–208.
28. Sahota, L.; Tiwari, G.N. Review on series connected photovoltaic thermal (PVT) systems: Analytical and experimental studies. *Sol. Energy* **2017**, *150*, 96–127. [[CrossRef](#)]
29. Kasaeian, A.; Khanjari, Y.; Golzari, S.; Mahian, O.; Wongwises, S. Effects of forced convection on the performance of a photovoltaic thermal system: An experimental study. *Exp. Therm. Fluid Sci.* **2017**, *85*, 13–21. [[CrossRef](#)]
30. Van Helden, W.G.J.; Van Zolingen, R.J.C.H.; Zondag, H.A. PV thermal systems: PV panels supplying renewable electricity and heat. *Prog. Photovolt. Res. App* **2004**, *12*, 415–426. [[CrossRef](#)]
31. Smith, M.K.; Selbak, H.; Wamser, C.C.; Nicholas, U.D.; Krieske, M.; Ssailor, D.J.; Rosenstiel, T.N. Water cooling method to improve the performance of field-mounted, insulated, and concentrating photovoltaic modules. *J. Sol. Energy Eng.* **2014**, *136*, 034503. [[CrossRef](#)]
32. Michael, J.J.; Iniyar, S. Performance of copper oxide/water nanofluid in a flat plate solar water heater under natural and forced circulations. *Energy Convers. Manag.* **2015**, *95*, 160–169. [[CrossRef](#)]
33. Matuska, T. Performance and economic analysis of hybrid PVT collectors in solar DHW system. *Energy Procedia* **2014**, *48*, 150–156. [[CrossRef](#)]
34. Nasrin, R.; Rahim, N.A.; Fayaz, H.; Hasanuzzaman, M. Water/MWCNT nanofluid based cooling system of PVT: Experimental and numerical research. *Renew. Energy* **2018**, *121*, 286–300. [[CrossRef](#)]
35. Abdelrazik, A.S.; Al-Sulaiman, F.A.; Saidur, R.; Ben-Mansour, R. A review on recent development for the design and packaging of hybrid photovoltaic/thermal (PV/T) solar systems. *Renew. Sustain. Energy Rev.* **2018**, *95*, 110–129. [[CrossRef](#)]
36. Michael, J.J.; Goic, R. Flat plate solar photovoltaic-thermal (PV/T) systems: A reference guide. *Renew. Sustain. Energy Rev.* **2015**, *51*, 62–88. [[CrossRef](#)]
37. Lari, M.O.; Sahin, A.Z. Design, performance and economic analysis of a nanofluid-based photovoltaic/thermal system for residential applications. *Energy Convers. Manag.* **2017**, *149*, 467–484. [[CrossRef](#)]
38. Maadi, S.R.; Kolahan, A.; Passandideh-Fard, M.; Sardarabadi, M. Effects of Nanofluids Thermo-Physical Properties on the Heat Transfer and 1st Law of Thermodynamic in a Serpentine PVT System. In Proceedings of the 17th Conference On Fluid Dynamics, Shahrood, Iran, 27–29 August 2017; pp. 1–14.
39. Said, Z.; Arora, S.; Bellos, E. A review on performance and environmental effects of conventional and nanofluid-based thermal photovoltaics. *Renew. Sustain. Energy Rev.* **2018**, *94*, 302–316. [[CrossRef](#)]
40. Da Silva, V.O.; Udaeta, M.E.M.; Gimenes, A.L.V.; Junior, A.C.d.; Linhares, A.L.; Rigolin, P.H.d. Development of Modular Cooling for Water-Cooled Photovoltaic Plant in Real Scale. In *Advanced Cooling Technologies and Applications*; IntechOpen: London, UK, 2018; p. 15.
41. Sultan, S.M.; Efzan, M.N.E. Review on recent Photovoltaic/Thermal (PV/T) technology advances and applications. *Sol. Energy* **2018**, *173*, 939–954. [[CrossRef](#)]
42. Lamnatou, C.; Chemisana, D. Photovoltaic/thermal (PVT) systems: A review with emphasis on environmental issues. *Renew. Energy* **2017**, *105*, 270–287. [[CrossRef](#)]
43. Han, H.; Wu, S.; Zhang, Z. Factors underlying rural household energy transition: A case study of China. *Energy Policy* **2018**, *114*, 234–244. [[CrossRef](#)]
44. Sawicka-chudy, P.; Sibiński, M.; Cholewa, M.; Klein, M.; Znajdek, K. Tests and theoretical analysis of a PVT hybrid collector operating under various insolation conditions. *Acta Innov.* **2018**, *26*, 62–74. [[CrossRef](#)]
45. Brötje, S.; Kirchner, M.; Giovannetti, F. Performance and heat transfer analysis of uncovered photovoltaic-thermal collectors with detachable compound. *Sol. Energy* **2018**, *170*, 406–418. [[CrossRef](#)]
46. Yuan, W.; Ji, J.; Li, Z.; Zhou, F.; Ren, X.; Zhao, X.; Liu, S. Comparison study of the performance of two kinds of photovoltaic/thermal(PV/T) systems and a PV module at high ambient temperature. *Energy* **2018**, *148*, 1153–1161. [[CrossRef](#)]
47. Yang, L.-H.; Liang, J.-D.; Hsu, C.-Y.; Yang, T.-H.; Chen, S.-L. Enhanced Efficiency of Photovoltaic Panels by Integrating a Spray Cooling System with Shallow Geothermal Energy Heat Exchanger. *Renew. Energy* **2018**, *134*, 970–981. [[CrossRef](#)]
48. Kelley, L.C. *The Design and Control of a Thermal Management System for a Photovoltaic Reverse Osmosis System*; Massachusetts Institute Technology: Cambridge, MA, USA, 2011.
49. Elnozahy, A.; Rahman, A.; Ali, A.; Abdel-Salam, M.; Ookawara, S. Performance of a PV module integrated with standalone building in hot arid areas as enhanced by surface cooling and cleaning. *Energy Build.* **2015**, *88*, 100–109. [[CrossRef](#)]
50. Klunth, A. Using Water as a Coolant to Increase Solar Panel Efficiency. In Proceedings of the California State Science Fair, Los Angeles, CA, USA, 19–20 May 2008.
51. Odeh, S.; Behnia, M. Improving Photovoltaic Module Efficiency Using Water Cooling. *Heat Transf. Eng.* **2009**, *30*, 499–505. [[CrossRef](#)]
52. Tabaei, H.; Ameri, M. Improving the effectiveness of a photovoltaic water pumping system by using booster reflector and cooling array surface by a film of water. *IJST Trans. Mech. Eng.* **2015**, *39*, 51–60.
53. Irwan, Y.M.; Leow, W.Z.; Irwanto, M.; Fareq, M.; Hassan, S.I.S.; Safwati, I.; Amelia, A.R. Comparison of solar panel cooling system by using dc brushless fan and dc water. *J. Phys. Conf. Ser.* **2015**, *622*, 1–11. [[CrossRef](#)]

54. Gagliano, A.; Tina, G.M.; Nocera, F.; Grasso, A.D.; Aneli, S. Description and performance analysis of a flexible photovoltaic/thermal (PV/T) solar system. *Renew. Energy* **2018**, 1–13. [CrossRef]
55. Das, D.; Kalita, P.; Roy, O. Flat plate hybrid photovoltaic-thermal (PV/T) system: A review on design and development. *Renew. Sustain. Energy Rev.* **2018**, *84*, 111–130. [CrossRef]
56. Wu, J.; Zhang, X.; Shen, J.; Wu, Y.; Connelly, K.; Yang, T.; Tang, L.; Xiao, M.; Wei, Y.; Jiang, K.; et al. A review of thermal absorbers and their integration methods for the combined solar photovoltaic/thermal (PV/T) modules. *Renew. Sustain. Energy Rev.* **2016**, *75*, 839–854. [CrossRef]
57. Heideier, R.B.; Gimenes, A.L.V.; Udaeta, M.E.M.; Saidel, M.A. Optical filter design applied to photovoltaic modules to maximize energy production. *Sol. Energy* **2018**, *159*, 908–913. [CrossRef]
58. KSB. *KSB Hydrobloc P500 Monofásica 220V, Data Sheet No. A2748/49.8P/6*; KSB: Frankenthal, Germany, 2007.
59. Da Silva, V.O.; Martinez-bolanos, J.R.; Heideier, R.B.; Gimenes, A.L.V.; Udaeta, M.E.M.; Saidel, M.A. Theoretical and experimental research to development of water-film cooling system for commercial photovoltaic modules. *IET Renew. Power Gener.* **2020**, 1–19. [CrossRef]
60. International Electrotechnical Commission. Photovoltaic System Performance Monitoring—Guidelines for Measurement, Data Exchange and Analysis-IEC 61724. 1998. Available online: https://webstore.iec.ch/preview/info_iec61724%7Bed1.0%7Den.pdf (accessed on 22 March 2017).
61. LogTeck Automação e Sistema. *Termoresistência PT100*; LogTeck Automação e Sistema: São Caetano do Sul, Brazil, 2017.
62. Novus. *Manual de Instruções Fieldlogger*; Novus: Canoas, Brazil, 2014.
63. SECON. Transdutores (Transmissores) de Tensão DC Modelo V420ADC. Available online: https://www.secon.com.br/pdf/181101051237_TRANSDUTOR-TENSAO-VDC.pdf (accessed on 10 April 2017).
64. SECON. Transdutores (Transmissores) de Corrente DC Modelo C420ADC. Available online: https://www.secon.com.br/pdf/181101050932_TRANSDUTOR-CORRENTE-CMI.pdf (accessed on 10 April 2017).
65. SECON. Transdutores de Potência Ativa Trifásica. Available online: https://www.secon.com.br/pdf/190130083951_TRANSDUTORES-POTENCIA-ATIVA.pdf (accessed on 10 April 2017).
66. IFM Eletronic. *Operating Instructions Mechatronic Flow Sensor*; IFM Eletronic: Essen, Germany, 2016.
67. Hukseflux. *Piranômetro Modelo: SR05-DA2-BL*; Hukseflux: Delft, The Netherlands, 2016.
68. Ammonit. Anemometer Thies First Class Advanced X S11200/ S11200H. 2018. Available online: https://www.ammonit.com/images/stories/download-pdfs/DataSheets/Anemometers/Anemometer_ThiesFirstClassAdvancedX_S11200-H.pdf (accessed on 11 April 2017).
69. NRG Systems. 110S TEMPERATURE SENSOR. Available online: <https://www.nrgsystems.com/products/met-sensors/other-met-sensors/detail/110s-temperature-sensor> (accessed on 3 April 2017).
70. NRG Systems. BP20 Barometric Pressure Sensor. Available online: <https://www.nrgsystems.com/products/met-sensors/other-met-sensors/detail/bp20-barometric-pressure-sensor> (accessed on 3 April 2017).
71. Gimenes, A.L.V.; Linhares, A.L.; Abreu, A.C., Jr.; Bernal, J.L.O.; Galvão, L.C.R.; Galvão, M.D.; Udaeta, M.E.M.; Kanayama, P.H.; Acebron, R.M.; Paula, R.V.; et al. Instrumental measurement of primary and secondary energy and systematization of big-data generated in a pilot eolic-solar system. *Espacios* **2018**, *39*, 22–38.
72. Nascimento, A.A.; Gimenes, A.L.V.; Linhares, A.L.; Abreu, A.C., Jr.; Bernal, J.L.O.; Spagiari, J.O.M.; Galvão, L.C.R.; Galvão, M.D.; Udaeta, M.E.M.; Rigolin, P.H.C.; et al. Design of the strategy for mass data from outdoor units of measurement of intermittent primary-energy quantities. *Espacios* **2018**, *39*, 24–43.
73. Relva, S.G.; Gimenes, A.L.V.; Udaeta, M.E.M.; Galvão, L.C.R. Transmittance index characterization at two solar measurement stations in Brazil. *Theor. Appl. Climatol.* **2020**, *139*, 205–219. [CrossRef]
74. Santana, J.R. *Clouds and Their Effects on Solar Radiation in São Paulo*; Universidade de São Paulo: São Paulo, Brazil, 2018.
75. Koffi, H.A.; Kakane, V.C.K.; Kuditcher, A.; Hughes, A.F.; Adeleye, M.B.; Amuzu, J.K.A. Seasonal variations in the operating temperature of silicon solar panels in southern Ghana. *Afr. J. Sci. Technol. Innov. Dev.* **2015**, *7*, 485–490. [CrossRef]
76. Sahli, M.; Correia, J.P.M.; Ahzi, S.; Touchal, S. Multi-physics modeling and simulation of heat and electrical yield generation in photovoltaics. *Sol. Energy Mater. Sol. Cells* **2018**, *180*, 358–372. [CrossRef]
77. Sharma, R.; Chong, A.P.; Li, J.B.; Aberle, A.G.; Huang, Y. Role of post-metallization anneal sequence and forming gas anneal to mitigate light and elevated temperature induced degradation of multicrystalline silicon solar cells. *Sol. Energy Mater. Sol. Cells* **2019**, *195*, 160–167. [CrossRef]
78. Gimenes, A.L.; Linhares, A.L.; Abreu, A.C., Jr.; Bernhard, D.B.; Bernal, J.L.; Udaeta, M.E.M.; Rigolin, P.H.C.; Acebron, R.M.; Carneiro, R.A.; Relva, S.G.; et al. Experimental development of cooling system addressing to photovoltaic power plant in real scale. *Espacios* **2018**, *39*, 49.
79. Tomar, V.; Tiwari, G.N.; Bhatti, T.S.; Norton, B. Thermal modeling and experimental evaluation of five different photovoltaic modules integrated on prototype test cells with and without water flow. *Energy Convers. Manag.* **2018**, *165*, 219–235. [CrossRef]
80. Climate-data.org. Climate Data for Cities Worldwide. 2018. Available online: <https://en.climate-data.org/> (accessed on 27 September 2019).
81. Kim, D.-J.; Kim, D.H.; Bhattara, S.; Oh, J.-H. Simulation and Model Validation of the Surface Cooling System for Improving the Power of a Photovoltaic Module. *J. Sol. Energy Eng.* **2011**, *133*, 041012. [CrossRef]

82. Buker, M.S.; Mempouo, B.; Riffat, S.B. Performance evaluation and techno-economic analysis of a novel building integrated PV/T roof collector: An experimental validation. *Energy Build.* **2014**, *76*, 164–175. [[CrossRef](#)]
83. Da Silva, V.O.; Udaeta, M.E.M.; Gimenes, A.L.V.; Linhares, A.L. Improving the Performance of Photovoltaic Power Plants with Determinative Module for the Cooling System. *Energy Power Eng.* **2017**, *9*, 309–323. [[CrossRef](#)]
84. Rahman, M.M.; Hasanuzzaman, M.; Rahim, N.A. Effects of operational conditions on the energy efficiency of photovoltaic modules operating in Malaysia. *J. Clean. Prod.* **2017**, *143*, 912–924. [[CrossRef](#)]
85. Osma-Pinto, G.; Ordóñez-Plata, G. Measuring the effect of forced irrigation on the front surface of PV panels for warm tropical conditions. *Energy Rep.* **2019**, *5*, 501–514. [[CrossRef](#)]
86. Lucas, M.; Ruiz, J.; Aguilar, F.J.; Cutillas, C.G.; Kaiser, A.S.; Vicente, P.G. Experimental study of a modified evaporative photovoltaic chimney including water sliding. *Renew. Energy* **2019**, *134*, 161–168. [[CrossRef](#)]